1936-1-T

ENGINEERING RESEARCH INSTITUTE
UNIVERSITY OF MICHIGAN•ANN ARBOR

INTERIM TECHNICAL REPORT

AN ANALYSIS OF UNDERWATER SOUND-TRANSMISSION DATA

by
J. R. FREDERICK
J. C. JOHNSON
W. H. KELLY

OFFICE OF NAVAL RESEARCH, U.S. NAVY DEPARTMENT
CONTRACT N6ONR-23221, ONR PROJECT NO. NR 261 008

April, 1954

Distribution List
Contract N6onr-232(21), NR 385-203

Chief of Naval Research
Acoustics Branch (Code 411)
Washington 25, D. C. (6 copies)

Chief of Naval Research
Undersea Warfare Branch (Code 466)
Washington 25, D. C. (1 copy)

Director,
Naval Research Laboratory
Technical Information Officer
Washington 25, D. C. (1 copy)

Commanding Officer
Office of Naval Research Branch Office
1030 E. Green Street
Pasadena 1, Calif. (1 copy)

Commanding Officer
Office of Naval Research Branch Office
10th Floor
The John Crerar Library Bldg.
86 E. Randolph St.
Chicago 1, Illinois (1 copy)

Commanding Officer
Office of Naval Research Branch Office
346 Broadway
New York 13, New York (1 copy)

Commanding Officer
Office of Naval Research Branch Office
1000 Geary Street
San Francisco, Calif. (1 copy)

Commanding Officer
Office of Naval Research
Navy 100, Fleet Post Office
New York, New York (1 copy)

Commanding Officer and Director
U. S. Navy Underwater Sound Laboratory
Fort Trumbull, New London, Conn. (1 copy)

Commanding Officer and Director
U. S. Navy Electronics Laboratory
San Diego 52, Calif. (1 copy)

Commander
Naval Air Development Center
Johnsville, Pa. (1 copy)

Chief,
Bureau of Ships (Code 847)
Navy Department
Washington 25, D. C. (1 copy)

Director
Marine Physical Laboratory
University of California
U. S. Navy Electronics Laboratory
San Diego 52, Calif. (1 copy)

Hudson Laboratories
Columbia University VIA ONR/New York
145 Palisades Street
Dobbs Ferry, New York (1 copy)

Lamont Geological Laboratory
Columbia University VIA ONR/New York
Torre Cliffs
Palisades, N. Y. (1 copy)

Woods Hole Oceanographic Institution
Woods Hole, Mass.
Attn: Mr. Vine (1 copy)

CONFIDENTIAL

ENGINEERING RESEARCH INSTITUTE
UNIVERSITY OF MICHIGAN
ANN ARBOR

INTERIM TECHNICAL REPORT

AN ANALYSIS OF UNDERWATER SOUND-TRANSMISSION DATA

By

J. R. FREDERICK

J. C. JOHNSON

W. H. KELLY

Project M936

OFFICE OF NAVAL RESEARCH, U.S. NAVY DEPARTMENT
N6onr-23221, ONR PROJECT NO. NR 261 008

April, 1954

CONFIDENTIAL

CONFIDENTIAL

ABSTRACT

Underwater sound-transmission data have been analyzed to determine the relative effects of various environmental parameters such as the depth of the surface isothermal layer, wind force, and thermal structure. Results are given for the effect of wind for a range on transmission loss in an isothermal layer for 8, 16, and 25 kc. The probable errors are 2, 3, and 4 db, respectively. Transmission-loss data vs. range for various combinations of projector and receiver depths expressed as multiples of half the layer depth are given. The principle of reciprocity has been found to be applicable in the analysis of the data. Correlation coefficients have been computed to determine the relative effects on transmission loss of factors such as wind force, bottom depth, and the thermal gradient below the layer. When analyzing data where a NAN thermal pattern is present, it has been found that a range unit related to the distance between the source and the shadow boundary decreases the spread of the data. In the analysis of shallow-water data from Woods Hole Oceanographic Institution it has been found that a range unit based on the bottom "skip" distance likewise reduces the spread of the data. Theoretical studies have been carried out which indicate that some information on the reflection coefficient of the sea surface may be obtained from an analysis of surface reflected pulse shapes. No data have been available to check this work as yet. Theoretical studies on the possible scattering caused by variations in the index of refraction of the medium are reported. The effect seems to be too small to be important, however. A theoretical expression is derived for computing values of scattering coefficients from transmission-loss data obtained in the shadow zone. They have been found to vary from 35 to 75 db.

INTERIM TECHNICAL REPORT

AN ANALYSIS OF UNDERWATER SOUND-TRANSMISSION DATA

I. INTRODUCTION

In the first six months of the present contract period various aspects of the underwater sound-transmission problem have been treated by the analysis of data obtained by other laboratories. In general the emphasis has been to find the effect of environmental factors on sound-transmission loss. The data used were from Project AMOS, UCDWR, WHOI, and NRL. The techniques of analysis that have been used include those developed in previous work under this contract.

The work has been divided into various tasks and some of the results obtained thus far are presented in this report.

II. CALCULATION OF THE PROBABLE ERRORS IN THE EMPIRICAL EQUATIONS FOR THE TRANSMISSION LOSS IN THE TOP HALF OF AN ISOTHERMAL LAYER

It has been found[1] that an empirical equation of the form,

$$L_A = \text{Adjusted loss} = A + B \log R_A + CR_A + DR_AW \quad ,$$

gives a good fit to transmission-loss data from Project AMOS and NRL. A, B, C, and D are constants that are determined by the method of least squares. Table I gives the equations previously reported. In the last column calculations were made only for the case of the projector and

[1] J. R. Frederick, and J. C. Johnson, "Study of Application of Environmental Information to the Detection Phase of Undersea Warfare", p.5-6, Engineering Research Institute Project M936, University of Michigan, Ann Arbor, December, 1953 (Confidential).

receiver in the top half of the surface isothermal layer. These equations were determined by the method of least squares over the adjusted range interval 0 to 1.5 skip distances. The NRL data are from references 2 and 3.

TABLE I

TABULATION OF THE EQUATION $L_A = A + B \log R_A + CR_A + DR_AW$ AS CALCULATED FROM THE ADJUSTED TRANSMISSION-LOSS DATA FOR 25, 16, AND 8 kc

Frequency, kc	Data Source	Line	N	Probable Error, db
25	AMOS Cruises 5,7,8,9,11	$L_A = 43.3 + 12.3 \log R_A + 15.2R_A + 3.1R_AW$	181	4.1
16	AMOS Cruises 5,7,8,9,11,12, and NRL	$L_A = 49.8 + 15.6 \log R_A + 4.5R_A + 2.1R_AW$	327	3.4
8	AMOS Cruises 5,7,8,9,11,12, and NRL	$L_A = 51.7 + 16.2 \log R_A + 0.9R_A + 1.1R_AW$	345	2.2

III. TRANSMISSION LOSS FOR VARIOUS COMBINATIONS OF TRANSMITTER AND RECEIVER DEPTHS

Figures 1, 2, 3, and 4 are curves showing the unadjusted and adjusted transmission loss at 8 and 25 kc for various combinations of projector and receiver depths. Only conditions where a surface isothermal layer was present have been considered. The projector or receiver depths were grouped according to whether they were in the upper half of the isothermal layer, the lower half of the layer, a distance below the layer equal to one-half the layer depth, or at all depths greater than these. The regions are designated as 1,2,3, and 4 and transmission from one region to another is indicated by 1-1, 1-2, 2-4, etc.

---

[2]R. J. Urick, "Sound Transmission Measurements at 8 and 16 kc in Caribbean Waters, Spring 1949", NRL Report 3556 (Confidential).

[3]R. J. Urick, "Sound Transmission to Long Ranges in the Ocean", NRL Report 3729 (1949) (Confidential).

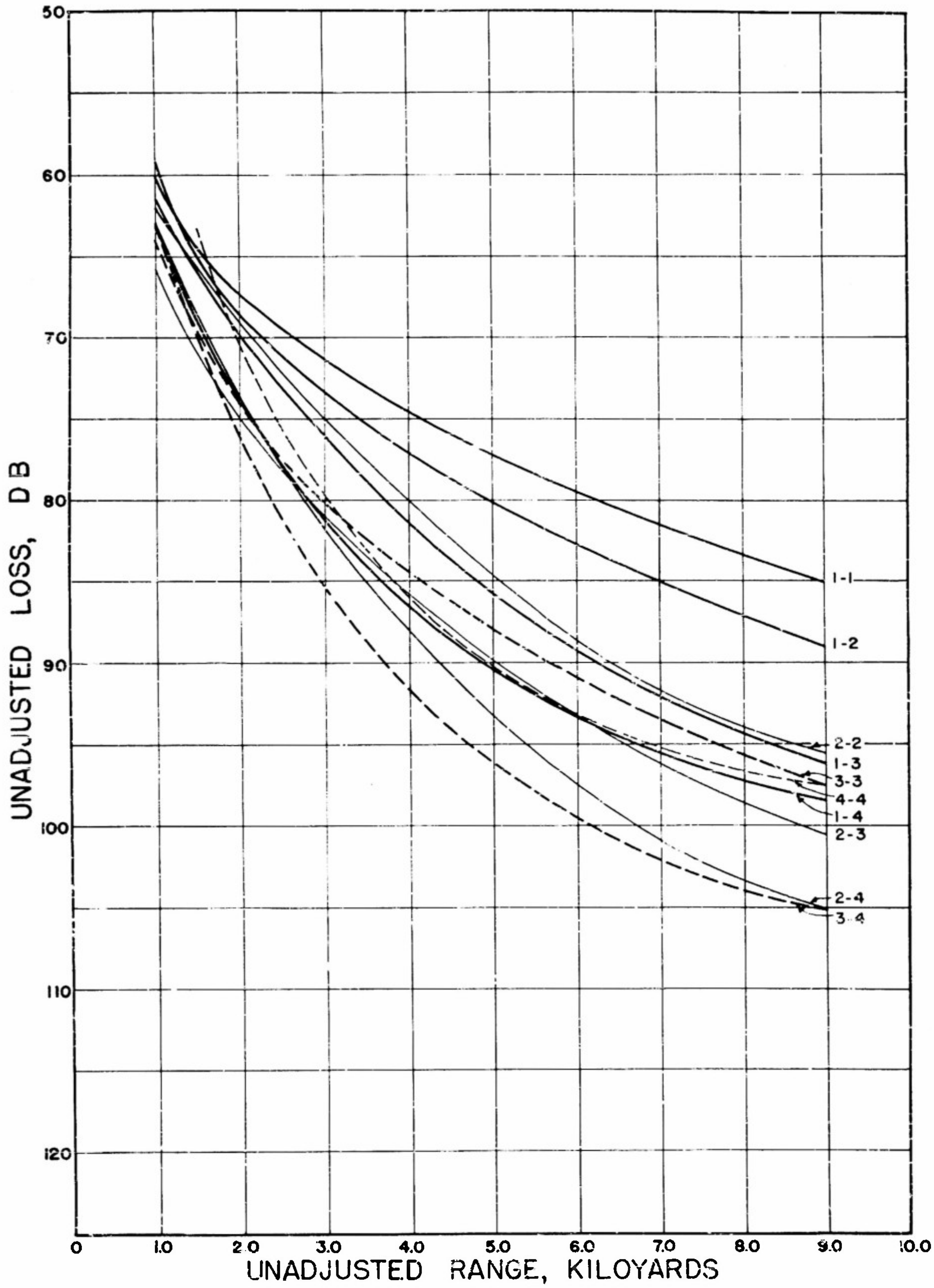

Fig. 1 Unadjusted Transmission Loss vs. Range for 8 kc for Various Combinations of Projector and Receiver Depths

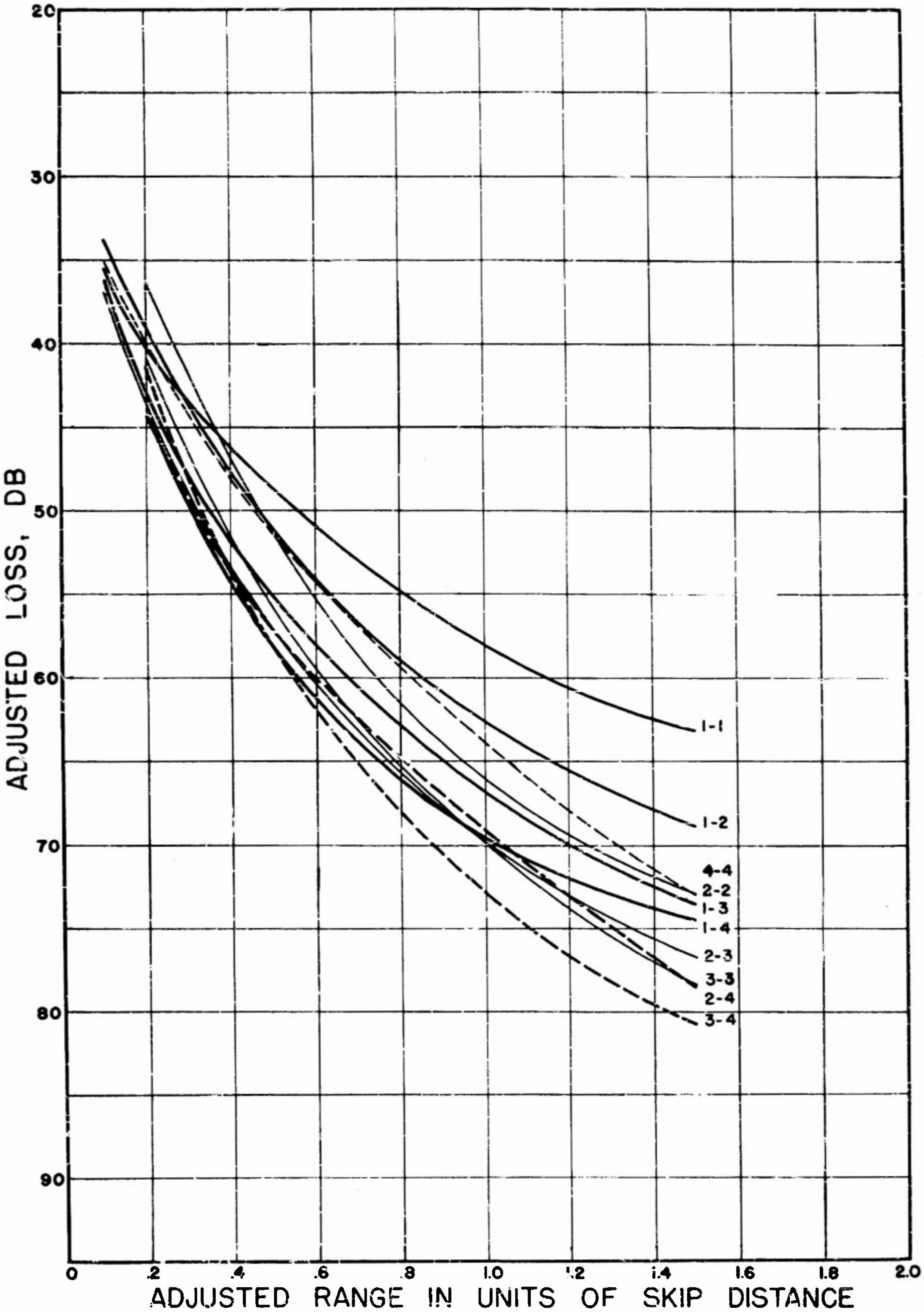

Fig. 2 Adjusted Transmission Loss vs. Adjusted Range for 8 kc for Various Combinations of Projector and Receiver Depths

CONFIDENTIAL

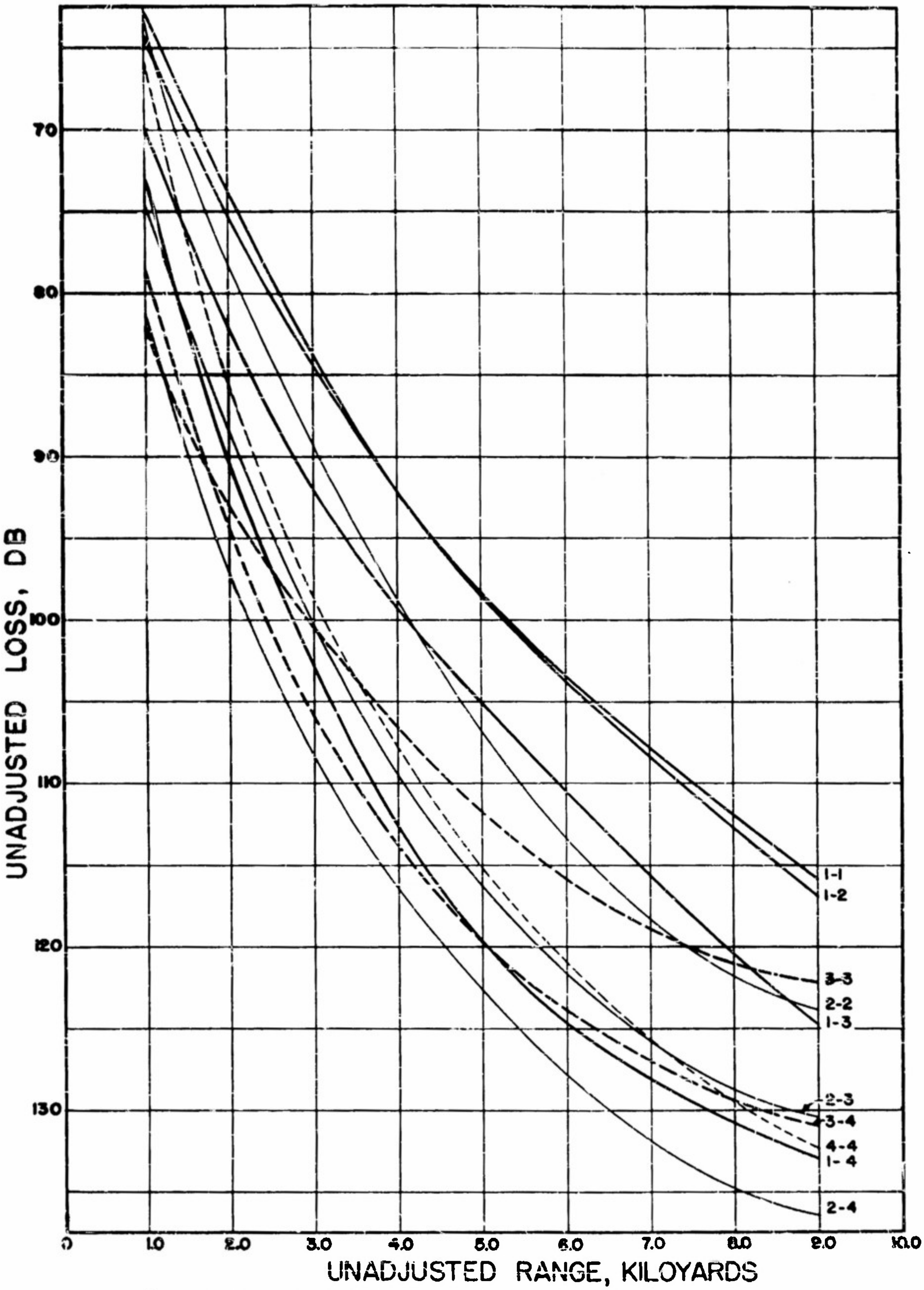

Fig. 3 Unadjusted Loss vs. Range for 25 kc for Various Combinations of Projector and Receiver Depths

CONFIDENTIAL

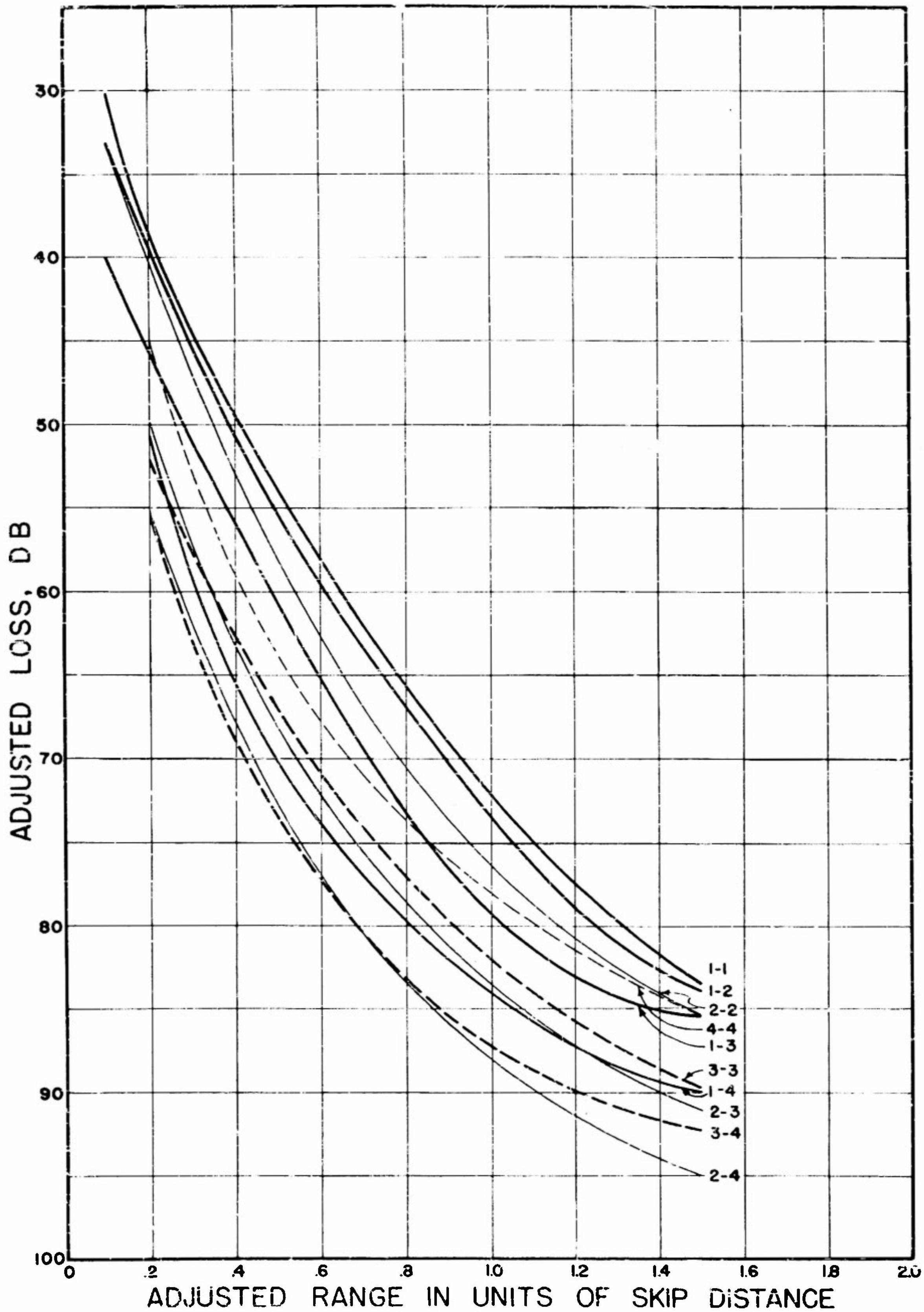

Fig. 4 Adjusted Loss vs. Adjusted Range for 25 kc for Various Combinations of Projector and Receiver Depths

Below the isothermal layer the only reason to expect the adjustment to work is that most of the energy arriving at a point below the layer arrives there after having travelled most of the distance in the layer, particularly at the longer ranges. It is to be expected that the adjustment will become progressively worse as the depth of the receiver and/or the projector below the layer is increased. Table II shows the probable errors for transmission between various regions.

TABLE II

PROBABLE ERRORS FOR TRANSMISSION-LOSS CURVES SHOWN IN FIGS. 1, 2, 3, AND 4

Transmission Path	Probable Errors, 8 kc, Unadjusted Data	Probable Errors, 8 kc, Adjusted Data	Probable Errors, 25 kc, Unadjusted Data	Probable Errors, 25 kc, Adjusted Data
1-1	5	3	8	4
1-2	5	3	8	5
1-3	4	4	8	6
1-4	4	4	8	7
2-2	6	6	8	6
2-3	8	5	10	8
2-4	5	3	8	7
3-3	6	6	12	9
3-4	6	6	8	10
4-4	6	5	8	9

In the plot of the transmission-loss data best lines were calculated only for the receiver and projector in the top half of the layer. In the other cases the lines were drawn to give the best fit to the plotted points. The data on which the curves are based are from Project AMOS, UCDWR and NRL.

Figure 5 shows a bar graph of the various ranges that are possible in the presence of an isothermal layer for different combinations of projector and target depths with respect to the layer depth. Arbitrary values of one-way transmission loss at 8 and 25 kc were assumed.

IV. LAW OF RECIPROCITY

If the law of reciprocity can be applied to the transmission of sound in the ocean, then interchanging the positions of the projector and receiver should have no effect on the observed transmission loss. An investigation of the extent to which it holds was made by comparing the results for the projector in the top half layer and the receiver in the first half-layer depth below the layer with the reciprocal situation where the receiver is in the top half of the layer and the projector in the first half-layer depth below the layer. Adjusted data from Cruises 5,7,8,9, and 11 in the range interval 0.3 to 1.5 skip distances were considered. The equations for the straight lines determined by the method of least squares over this interval are given in Table III. These lines were calculated over the adjusted range interval of 0.3 to 1.5 skip distances. R_A is the adjusted range.

TABLE III

EQUATIONS OF THE STRAIGHT LINES DETERMINED BY THE METHOD OF LEAST SQUARES FOR RECIPROCAL POSITIONS OF THE PROJECTOR AND THE RECEIVER

Frequency, kc	Adjusted Projector Depths	Adjusted Receiver Depths	Adjusted Transmission Loss, db	No. of Measurements
25	0 - 0.5	1.0 - 1.5	$42.3 + 34.6R_A$	99
25	1.0 - 1.5	0 - 0.5	$44.0 + 35.2R_A$	47
8	0 - 0.5	1.0 - 1.5	$44.3 + 21.1R_A$	98
8	1.0 - 1.5	0 - 0.5	$42.8 + 25.3R_A$	47

The agreement between the reciprocal cases is good and hence it appears that the law of reciprocity can be applied to transmission under these conditions.

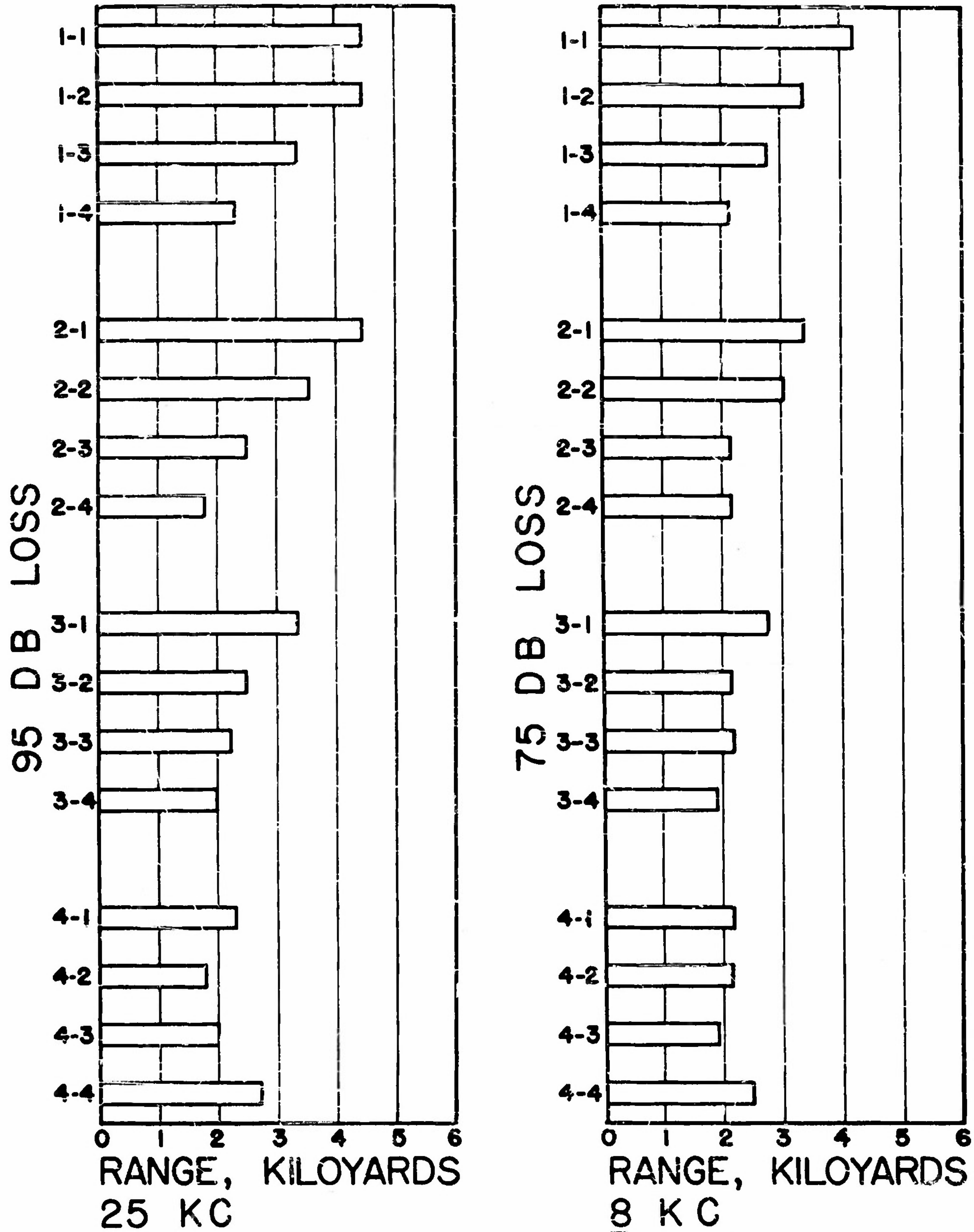

Fig. 5 Bar Graphs Showing Various Ranges that are Possible in the Presence of a Surface Isothermal Layer for Different Combinations of Projector and Target Depths with Respect to the Layer Depth. Arbitrary Values of Allowed One-way Transmission Loss at 8 and 25 kc are Assumed, Namely 75 and 95 db, Respectively.

V. CORRELATION OF UNDERWATER SOUND-TRANSMISSION LOSS WITH VARIOUS ENVIRONMENTAL CONDITIONS

In order to determine the relative importance of some of the factors affecting underwater sound transmission, a study has been made of the transmission-loss data obtained by project AMOS, UCDWR and NRL. The procedure has been to calculate the correlation coefficients between transmission loss and the magnitude of various environmental factors which are known.

Only transmission-loss data with an isothermal layer present have been considered. The quantitative effects of layer depth and temperature of the layer have already been shown in a previous report.[4] When the data are adjusted for variations in layer depth and temperature the spread becomes much less and a measure of the effects of the other factors such as wind force, the gradient below the layer, transducer depth, etc., are more easily obtained.

As is shown in reference 1 the adjusted transmission loss is obtained from the observed loss by means of the following formulas

$$L_A = L_o - \alpha_T R_U - 10 \log D ,$$

where

L_A = adjusted transmission loss, db,

L_o = observed transmission loss, db,

$\alpha_T = \dfrac{Af_m f^2}{f_m^2 + f^2}$, the relaxation absorption coefficient, db/kyd,

with

$f_m = 2.19 \times 10^7 \exp -\left(\dfrac{6300}{t + 460}\right)$,

$A = 0.60$,

t = temperature °F ,

[4] W. C. Meecham, J. C. Johnson, J. R. Frederick, "An Analysis of Project AMOS Data to Determine the Effects of Oceanographic Conditions on 8 and 25 kc Sound Transmission", Engineering Research Institute Project M936, University of Michigan, Ann Arbor, March, 1953 (Confidential).

R_U = unadjusted range in kiloyards, and

D = layer depth in feet.

The resulting adjusted transmission loss L_A can be expressed empirically by an equation of the form

$$L_A = A + B \log R_A + CR + DR_A W ,$$

where A, B, C, and D are constants determined by the method of least squares fit, W, is the wind force in Beaufort units, and R_A is the adjusted range. R_A is obtained by means of the following equation

$$R_A = \frac{R_U}{492 \sqrt{D}} .$$

The adjusted projector and receiver depths are obtained by dividing the unadjusted depths by the layer depth.

At adjusted ranges greater than 0.2 or 0.3 the dependence of transmission loss on range is approximately linear, and hence, to reduce the amount of calculations most of the correlation coefficients presented in this report have been computed using a straight line to represent the average loss in this region. The principal range dependence of the adjusted loss is removed by subtracting the average loss from the observed loss at a given range. This difference is referred to as the deviation of adjusted loss from the best line. It is this deviation that is correlated with the various environmental factors.

Standard statistical methods and concepts were used in the determination of the correlations.[5]

Data at 25, 16, and 8 kc from project AMOS Cruises 5, 7, 8, 9, 10, 11, and 12 and from UCDWR[6] are used. However, most of the calculations only make use of AMOS data. Table IV lists the AMOS stations that were used and the wind forces, layer depths, and surface temperatures of those stations.

Only projector depths in the upper half of the isothermal layer were used. Hydrophone depths are grouped according to whether they are

---

[5] C. H. Goulden, Methods of Statistical Analysis, 2nd Ed., John Wiley and Sons, New York, 1952.

[6] "Transfer of UCDWR Underwater Sound Propagation Data to IBM Punched Cards by USNUSL", USNUSL Tech. Memo. NP24/21A1, 5 November 1951.

TABLE IV

PROJECT AMOS CRUISES AND STATIONS USED IN THE CALCULATION OF CORRELATION BETWEEN TRANSMISSION LOSS AND VARIOUS ENVIRONMENTAL PARAMETERS

Cruise	Station	Wind Force, Beaufort Units	Layer Depth, ft	Surface Temperature °F
5	4	3.5	132	79
5	4	4.0	132	79
5	5	4.0	154	79
5	6	5.0	269	78
5	6	5.5	269	78
5	7	4.0	255	76
5	20	4.5	121	71
5	21	4.5	97	69
5	23	2.5	42	70
5	23	3.5	42	70
5	25	4.5	97	69
5	25	6.0	97	69
7	5	2.5	125	81
7	8	4.5	225	76
7	8	5.0	225	76
8	1	1.0	450	68
8	1	1.5	450	68
8	1	3.0	450	68
8	1	4.0	450	68
8	3	3.0	390	69
8	3	4.0	390	69
8	3	4.5	390	69
8	4	0.5	360	69
8	4	1.0	360	69
8	4	2.0	360	69
8	7	3.0	490	69
8	7	3.5	490	68
8	7	3.5	620	68
8	9	0	670	63
8	9	0.5	670	63
8	10	0.5	640	63
8	10	1.0	640	63
8	23	2.5	125	65

TABLE IV (Continued)

Cruise	Station	Wind Force Beaufort Units	Layer Depth, ft	Surface Temperature, °F
8	23	3.0	125	65
8	23	3.5	125	65
9	5	6.0	95	51
9	5	6.5	95	51
9	6	2.0	60	49
9	6	3.5	109	49
9	6	4.0	109	49
9	6	4.0	60	49
9	7	3.5	54	50
9	7	4.0	54	50
9	8	4.0	55	51
9	10	1.0	85	58
9	10	2.0	85	58
9	10	4.0	85	58
9	11	2.5	65	65
9	12	4.0	75	67
9	12	5.0	75	67
9	15	3.5	65	67
9	16	6.0	95	64
9	17	3.0	125	62
9	17	4.0	125	62
9	18	5.0	85	60
9	18	5.5	85	60
11	2	4.5	65	47
11	2	5.0	65	47
11	2	5.5	65	47
11	3	4.5	45	45
11	3	5.0	75	44
11	3	5.5	75	44
11	4	2.5	45	46
11	4	3.0	65	46
11	4	4.0	65	46
11	5	3.5	45	49
11	17	2.0	65	51
11	18	3.0	55	59

in the upper or lower half of the layer or below the layer. The transmission losses used are averages of the transmission losses taken in a hydrophone depth interval at a given range.

Considering that the data studied represent a random sample of the effects present in the ocean, the results presented here can be regarded as valid. Occasionally there are instances where even though there were many measurements this condition of randomness is probably not sufficiently fulfilled because the number of stations considered was not large enough. In these cases anomalous results may be expected. In general, however, the correlation coefficients obtained are in agreement with the mechanisms involved in transmission loss that have been postulated.

A. The Effect of Wind Force on Transmission Loss

When there is transmission in a channel produced by a surface isothermal layer one of the contributing causes to the loss is scattering from the layer by the surface and by oceanographic phenomena related to the surface. This means that the loss would be expected to increase with an increase in the surface roughness or sea state. Since sea state is just an estimate by an observer and hence not too reliable, it was felt that the wind force, a measureable quantity, would be a better description of the sea surface. A finite and positive correlation between the wind force and the deviations of the adjusted transmission loss would be expected from the best straight line fitting the data. It is found that this correlation coefficient at 25 kc for the projector and receiver in the top half of the layer is + 0.50, which is significant at the 1 percent level for the 118 measurements taken from AMOS Cruises 5, 7, 8, 9, 10, and 11 in the adjusted range interval 0.4 to 1.1 skip distances (the linear portion of the curve).

In a report by Munk[7] it is stated that certain phenomena noted at sea show a "discontinuity" at a wind speed of about 7 meters per second, which corresponds to a Beaufort 4 wind force. Among these phenomena mentioned are the number of white caps, wind stress, rate of evaporation, sea return on a radar screen, etc. In an earlier report by this group[4] it was mentioned that the deviations of the adjusted transmission loss from the line of least squares could be grouped around two different ordinates with a transition occurring at about wind force 3, e.g., a curve of the form shown in Fig. 6 could be fitted to the data.

Since the calculation of the correlation coefficients used in this study assumes a linear dependence between the variables, it might be expected

---

[7] W. H. Munk, "A Critical Wind Speed for Air-Sea Boundary Processes", New Series, No. 349, Scripps Institute of Oceanography.

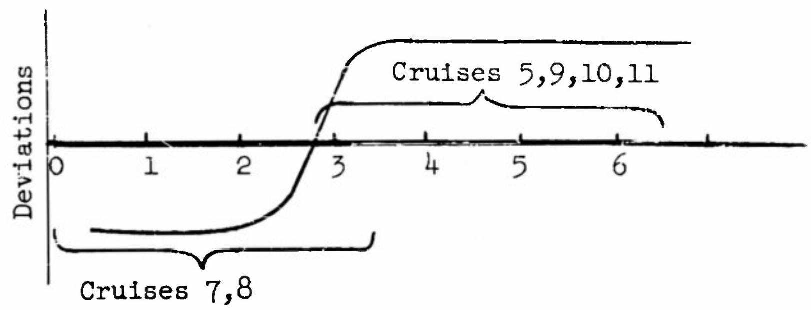

Fig. 6

Deviations of Adjusted Transmission Loss from the Line of Least Squares vs. Wind Force

that the presence of the above effect could be emphasized by grouping the data into smaller groups according to wind force and determining the correlation coefficients. In general, it was found that the wind forces for the stations used from AMOS Cruises 7 and 8 were low and were spread over both regions of the curve shown in Fig. 6. The wind forces from Cruises 5, 9, 10, and 11 on the other hand, were mainly over the upper part of the curve. If there is a wind force effect on transmission loss, then because of the distribution of wind forces the correlation of the deviations of the adjusted loss vs. wind force, r_{dAW}, would be higher for Cruises 7 and 8 than that for Cruises 5, 8, 10, and 11. Thus the coefficient for all the data would intermediate between these two groups. This turns out to be the case as can be seen in Table V.

To check on the reliability of the AMOS data calculations were made for the wind-force effect using UCDWR data obtained in the Pacific Ocean from 1944 to 1945. It was found that the two groups of data gave consistent results for the wind-force correlations. For 24 kc data in the range interval 0.20 to 1.10 with the receiver in the top half of the layer, 352 UCDWR measurements gave a correlation coefficient between transmission loss and wind force of 0.47. This is significant at the 1 percent level for this amount of data. This is to be compared with a correlation of 0.52 which was significant at the 1 percent level for 150 AMOS points in the same range and depth intervals.

Since the sound at the longer ranges has been reflected from the surface more times than that at shorter ranges, it would be expected that the inclusion of the range 1.10 to 1.50 in Table V for Cruises 5, 9, 10, and 11 would tend to make the correlation higher than it would otherwise.

TABLE V

CORRELATION COEFFICIENT FOR DEVIATIONS OF THE 25 kc ADJUSTED TRANSMISSION LOSS FROM THE STRAIGHT LINE OF LEAST SQUARES FITTING THE DATA vs. WIND FORCE

Both the projector and receiver were in the top half of the layer

Cruises	Range Interval, Skip Distances	Correlation between Transmission Loss and Wind Force	N	Significance Level, %
7,8	0.40 - 1.10	0.64	46	1
5,9,10,11	0.40 - 1.50	0.23	88	5
5,7,8,9,10,11	0.40 - 1.10	0.53	118	1

The fact that this correlation coefficient is small probably results from the poor distribution of the wind forces.

The distribution of the data is poor from another standpoint. The high wind-force data, in general, has shallower layers than the low wind-force data. How much of the above mentioned effect is due to wind force and how much of it is actually due to layer depth cannot be completely answered by the use of AMOS data. It is significant, therefore, that the UCDWR data gave similar correlations.

B. The Influence of Range on the Effect of Wind Force on Transmission Loss

As mentioned above, a larger percentage of the energy at the longer ranges has been reflected from the surface, and hence the influence of range on the wind-force effect will be larger at the longer ranges. It has been shown[8,9] that this effect on intensity is approximately exponential

[8] W. C. Meecham, "Propagation of Radiation in an Inhomogeneous Medium Near an Irregular Surface", JASA 25, 1012 (1953).

[9] W. C. Meecham, "Memorandum on the Attenuation of Sound in the Ocean at Large Ranges due to Surface Reflection", Memorandum submitted to ONR, December, 1953.

with ranges and so the deviations in db were divided by the corresponding adjusted ranges in order to reduce the bias of the longer ranges. The correlation coefficients, r_{d_{AW}/R_A}, were then recalculated for this ratio and wind force and found not to be significantly different.

As a further attempt to study the influence of range on the wind-force effect the range dependence was partialled out.* The result was that the correlation coefficient again was not significantly changed. The fact that the calculation of these coefficients assumes that all the dependences are linear, coupled with the fact that no significant changes were noted after partialling out the range, leads to the inference that this influence, to a first approximation, is not linear.

C. The Frequency Dependence of the Effect of Wind Force

In general, as the wavelength is increased it is expected that the surface and surface connected effects will become less and less important, i.e., the scattering cross section decreases. However, as may be seen in Table VI the correlation at 8 kc is almost as large as that at 25 kc. The data are for both the projector and receiver in the top half of the layer. The apparent anomaly at 16 kc can be associated with the general tendency of the AMOS data at that frequency to give spurious results in other respects. Results for the receiver in other positions are given in Table VII.

TABLE VI

CORRELATION COEFFICIENTS FOR DEVIATIONS OF THE ADJUSTED TRANSMISSION LOSS FROM THE STRAIGHT LINE OF LEAST SQUARES vs. WIND FORCE

Frequency, kc	Cruises	Range	$r_{d_{AW}}$	Significance Level, %
25	8	0.4 - 1.1	0.6	1
25	5,7,8,9,10,11	0.4 - 1.1	0.5	1
16	5,9,10,11	0.4 - 1.1	0.3	1
16	8	0.4 - 1.1	0.03	-
8	5,7,8,9,11	0.4 - 1.1	0.4	1
8	8	0.4 - 1.1	0.5	1

*Partialling out range dependence means that an assumed linear dependence of the deviations on range is removed by the calculation of the partial correlation coefficient.

D. Effect of Wind Force on Transmission Loss to the Region Below Isothermal Layer

In the model used the energy radiated from a projector in an isothermal layer to a receiver below the layer travels to that point mostly by the way of the layer, subsequently arriving there after having been scattered by the surface and surface connected effects. The effect of the wind force on the deviations would, therefore, be approximately the same as that shown in Table VI for transmission in an isothermal layer. Table VII shows this to be the case, particularly at 25 kc. The means were calculated for adjusted transmission loss in the range interval of 0.1 skip distance. The projector was in the top half layer, the receiver in the first half-layer depth below the layer.

TABLE VII

CORRELATION COEFFICIENTS FOR THE AMOS CRUISES 8 AND 9 DEVIATIONS OF THE ADJUSTED TRANSMISSION LOSS FROM THE MEANS OF AMOS CRUISES 5,7,8,9, AND 11 vs. WIND FORCE

Frequency, kc	Range	$r_{d_A W}$	N	Significance Level, %
25	0.4 - 1.1	0.66	41	1
16	0.4 - 1.1	0.13	38	-
8	0.4 - 1.1	0.34	41	5

The reason for the use of the deviations of Cruises 8 and 9 from the means of Cruises 5,7,8,9, and 11 is that at the time these were calculated the BTs for the other Cruises were not available. They were later obtained when they were needed to determine the effect of the gradient below the layer, which is discussed below.

E. The Effect of the Gradient Below the Layer on the Wind-Force Effect

The general shape of the thermal pattern of the cases considered on this study is shown in Fig. 7. The slope of the initial break, i, was chosen as one simple measure of the thermal gradient beneath the layer. This is defined as the slope of the thermal pattern immediately beneath the layer in units of degrees per hundred feet. Two other measures were also

used: ΔT_{50} = average slope in first 50 feet below the layer and ΔT_{100} = average slope in first 100 feet below the layer. It was found that the use of these different measures gave about the same results for each case because of the high correlation between these three measures.

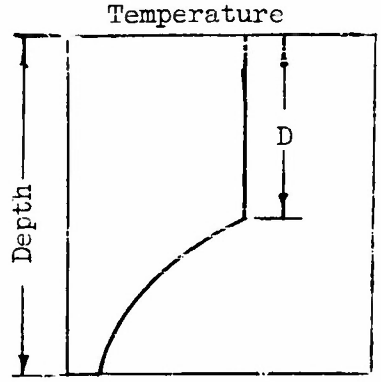

Fig. 7

Typical Bathythermogram for
an Isothermal Surface Layer

The general technique used in this section was to partial out the effect of the thermal gradient, assuming strictly linear dependences. The results obtained are given in Table VIII, where $r_{d_{AW}}$ and $r_{d_{AW}.i}$ are the coefficients before and after partialling out the slope of the initial break. The data used were in the adjusted range interval 0.4 to 1.1 skip distances.

Using the thermal information from all the cruises, the results in Table IX were obtained using ΔT_{100} as the measure of the gradient beneath the layer. The projector was in the top half of the layer while the receiver was in the first 150 feet below the layer. The calculations were made over the adjusted range interval 0.3 to 1.5 skip distances. Data from AMOS Cruises 5,7,8,9, and 11 were used.

Since the correlation coefficients are not significantly changed when the gradient below the layer is taken into account by partialling it out, the conclusion may be drawn that it has little effect on the magnitude of the wind-force effect for both the projector and receiver in the top half layer. It is a slightly larger effect for the receiver beneath the layer, as might be expected.

TABLE VIII

THE CORRELATION COEFFICIENTS OF THE DEVIATIONS OF CRUISES 8 AND 9 ADJUSTED TRANSMISSION-LOSS DATA FROM THE MEANS OF CRUISES 5,7,8,9, AND 11 vs. WIND FORCE

Frequency, kc	Receiver Depth	$r_{d_A W}$	Significance Level, %	$r_{d_A W \cdot i}$	Significance Level, %	N
25	top half of layer	0.63	1	0.55	1	78
25	first half-layer depth below the layer	0.66	1	0.57	1	41
16	first half-layer depth below the layer	0.13	-	0.13	-	38
8	top half of layer	0.39	1	0.35	1	79
8	first half-layer depth below the layer	0.34	5	0.15	-	41

TABLE IX

CORRELATION COEFFICIENTS OF THE DEVIATION OF THE ADJUSTED TRANSMISSION LOSS FROM THE STRAIGHT LINE OF LEAST SQUARES vs. WIND FORCE BEFORE, $r_{d_A W}$, AND AFTER PARTIALLING OUT ΔT_{100} $r_{d_A W \cdot \Delta T_{100}}$

Frequency, kc	Layer Depth, ft	$r_{d_A W}$	$r_{d_A W \cdot \Delta T_{100}}$	N	Significance Levels, %	
25	$D < 130$	0.51	0.37	44	1	5
25	$D > 130$	0.75	0.69	70	1	1
8	$D > 130$	-0.28	-0.39	70	-	1
8	$D < 130$	0.60	0.47	43	1	1

F. Effect of Layer Temperature, Bottom Depth, and Layer Depth on the Wind-Force Effect

In order to show that the effect of wind force on the transmission loss was not caused by variations in surface temperature, bottom depth, or layer depth, correlation coefficients were computed with these quantities partialled out. The results were not significantly different. There were slight increases in the correlation coefficient when the effects of surface temperature and bottom depth were removed and a slight decrease when variations in layer depth were taken into consideration.

G. Correlation of Deviations of Adjusted Loss with Range

Because of the many effects entering into the transmission of sound that tend to increase the spread of the measured loss with range it is expected that there would be a strong correlation between the deviations of the adjusted loss with range. This is borne out by the calculations. This correlation coefficient was calculated at 25 kc for stations from Cruise 8 with both projector and receiver in the top half of the layer. The range interval considered was 0.4 to 1.1 skip distances. The value found was 0.76, which for the 46 points used is significant at the 1 percent level. It was also found that the partialling out of the wind force increased this coefficient to 0.84, also significant at the 1 percent level.

H. Correlation of the Deviations of the Adjusted Loss vs. Bottom Depth

No significant correlation was found to exist between transmission loss and bottom depth over the ranges of 0.2 to 1.5 skip distances considered in this investigation. Only transmission from a projector in the top half of the layer to a receiver in the first half-layer depth below the layer were considered in making this analysis.

I. Correlations of the Deviations of the Adjusted Loss vs. the Gradient Below the Layer

Since the sound that is measured in the layer at a given range travels almost entirely to that point by way of the isothermal layer, it might be expected that the transmission loss in the layer would not be dependent on the gradient below the layer. When the wind force was partialled out, it was found in most cases that the correlation coefficient was decreased almost to zero. Table X gives the results obtained for the various correlation coefficients. The coefficients were calculated over

the adjusted range interval 0.4 to 1.1 skip distances. The projector and receiver were in the top half of the layer. In general, the agreement and consistency is good.

TABLE X

THE CORRELATION COEFFICIENTS OF THE DEVIATIONS OF THE ADJUSTED LOSS FROM THE STRAIGHT LINE OF LEAST SQUARES vs. THE SLOPE OF THE INITIAL BREAK BEFORE AND AFTER PARTIALLING OUT WIND FORCE

Frequency, kc	Cruises	r_{dAi}	Partial Out	N	Significance Level, %
25	8	0.06		58	-
25	8	0.01	wind force	58	-
25	8,9	0.41		78	1
25	8,9	0.07	wind force	78	-
8	8	0.45		58	1
8	8	0.46	wind force	58	1
8	8,9	0.19		79	-
8	8,9	0.05	wind force	79	-

Table X was calculated using the slope of the initial break as the measure of the gradient below the layer. It was found, as has been mentioned before, that the other two measures of the gradient below the layer (ΔT_{50} and ΔT_{100}) lead to essentially the same results.

For transmission from a projector in the layer to a receiver below the layer a positive correlation between the deviations and the gradient below the layer might be expected. This is partially because for a sharper gradient the stronger the refraction, and hence, a smaller region in the layer is scattering energy from the layer into the region below, therefore a larger loss would be noted. Table XI calculated from data from AMOS Cruises 8 and 9 in the adjusted range interval 0.4 to 1.1 skip distances shows this to be the case. These correlation coefficients are all significant at the 1 percent level. The projector was in the top half of the layer and the receiver was in the first half-layer depth below the layer.

TABLE XI

CORRELATION COEFFICIENT OF THE DEVIATIONS OF THE ADJUSTED TRANSMISSION LOSS FROM THE STRAIGHT LINE OF LEAST SQUARES vs. THE SLOPE OF THE INITIAL BREAK BEFORE AND AFTER PARTIALLING OUT WIND FORCE

Frequency, kc	$r_{d_A i}$	N	Partial Out
25	0.72	41	
25	0.66	41	wind force
16	0.52	38	
16	0.52	38	wind force
8	0.51	41	
8	0.43	41	wind force

Table XII gives similar results for the AMOS Cruises 5,7,8,9, and 11 with the receiver in the first 150 feet below the isothermal layer and the projector in the top half of the surface isothermal layer. These are calculated over the range interval 0.3 to 1.5 skip distances. It is to be noted that the partialling out of the wind force decreases the correlation between the deviations and the gradient beneath the layer.

The correlation is, in most cases, significantly smaller for the deep layers than that for the shallow layers. This difference in correlation coefficients for the different groupings of layer depths might be attributed in part to the fact that for the deeper layers the gradients tend to be less sharp. Hence, the distribution is such that these gradients do not vary as much as those for the shallow layers. This could therefore result in a smaller correlation coefficient for the deeper layers.

TABLE XII

CORRELATION COEFFICIENTS OF DEVIATIONS OF THE ADJUSTED LOSS vs. A MEASURE OF THE THERMAL GRADIENT BELOW THE LAYER BEFORE AND AFTER PARTIALLING OUT WIND FORCE

Frequency, kc	Layer Depth	$r_{d_A i}$	$r_{d_A \Delta T_{100}}$	Partial Out	N	Significance Level, %	
25	D < 130	0.54	0.57		44	1	1
25	D < 130	0.38	0.47	wind force	44	1	1
25	D > 130	0.29	0.47		70	5	5
25	D > 130	0.26	0.26	wind force	70	5	5
16	D < 130	0.41	0.47		41	1	1
16	D > 130	0.18	0.18		66	-	-
8	D < 130	0.56	0.52		43	1	1
8	D < 130	0.34	0.34	wind force	43	5	5
8	D > 130	0.50	0.16		70	1	
8	D > 130	0.58	0.32	wind force	70	1	1

VI. ANALYSIS OF TRANSMISSION LOSS DATA WHEN A NEGATIVE GRADIENT IS PRESENT

The analysis of transmission loss in water with negative gradients extending down from the surface was undertaken using data obtained from the AMOS Cruises. The useable amount of the data limits the analysis to a qualitative explanation of the phenomena observed. The effects of the environmental conditions such as wind force, sea state, and small variations in the thermal gradient were not considered.

Six stations, listed in Table XIII, with definite negative gradients were selected from AMOS Cruises for analysis.

TABLE XIII

AMOS STATIONS USED IN NEGATIVE GRADIENT ANALYSIS

Cruise	Station	Depth Interval, ft	Temperature Gradient, °F/100 ft
5	22	surface downward	1
8	22	surface downward	0.5
9	9	surface to 155	0.7
		155 to 200	11.6
		200 downward	0.85
11	8	surface to 150	3
		150 downward	0.7
11	11	surface to 85	2
		85 to 120	10
		120 downward	1.3
11	13	surface to 110	1.4
		110 to 145	9
		145 downward	0.5

Projector depths of 20, 50, 100, 150, 200, and 250 feet were used. Then the data were grouped according to whether the receiver depths were shallow (20 and 50 feet) or deep 200 and 250 feet).

To reduce the spread of the data, the observed range was expressed in R_O units; R_O being defined in Fig. 8 for an arbitrary ray diagram, which is the horizontal range between the projector and the position of the surface limited ray at an arbitrary depth of 100 feet. It is probable that some other depth more closely related to the receiver depth would give better adjustment of the data, but this adds to the complexity of the

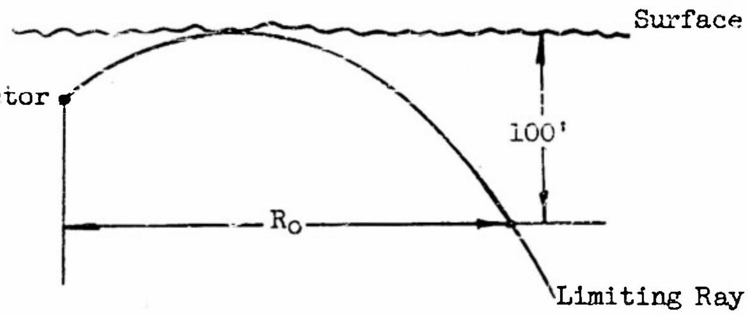

Fig. 8

Limiting Ray for Transmission in Negative Gradient Water, R_o is the Range Unit in which to Express the Observed Ranges

analysis. Projector depths were not averaged, but a separate ray diagram was made for each one.

The usual temperature dependent relaxation loss α_T was subtracted from the measured loss. The temperature used was an approximate average over the ray path between the projector and receiver. Figures 9 through 13 show plots of the unadjusted and adjusted data.

By examination of the plotted data the following conclusions may be drawn:

1. Adjustment of 25 kc data results in a noticeable decrease in the spread of the data.

2. There appears to be no abrupt increase in the rate at which the attenuation is increasing on going from the direct field into the shadow zone. It should be noted, though, that the range unit chosen is only an approximation of the range to the shadow boundary.

3. Background noise appears to limit the measurable intensity, and hence, the measurable loss at distances greater than 1.5 to 2.0 units.

A larger amount of data would allow future analyses to consider effects of wind force and other environmental data. It would also be possible with more data to obtain an empirical expression for the transmission loss in terms of the projector and receiver depths and the average temperature gradient over the region of interest.

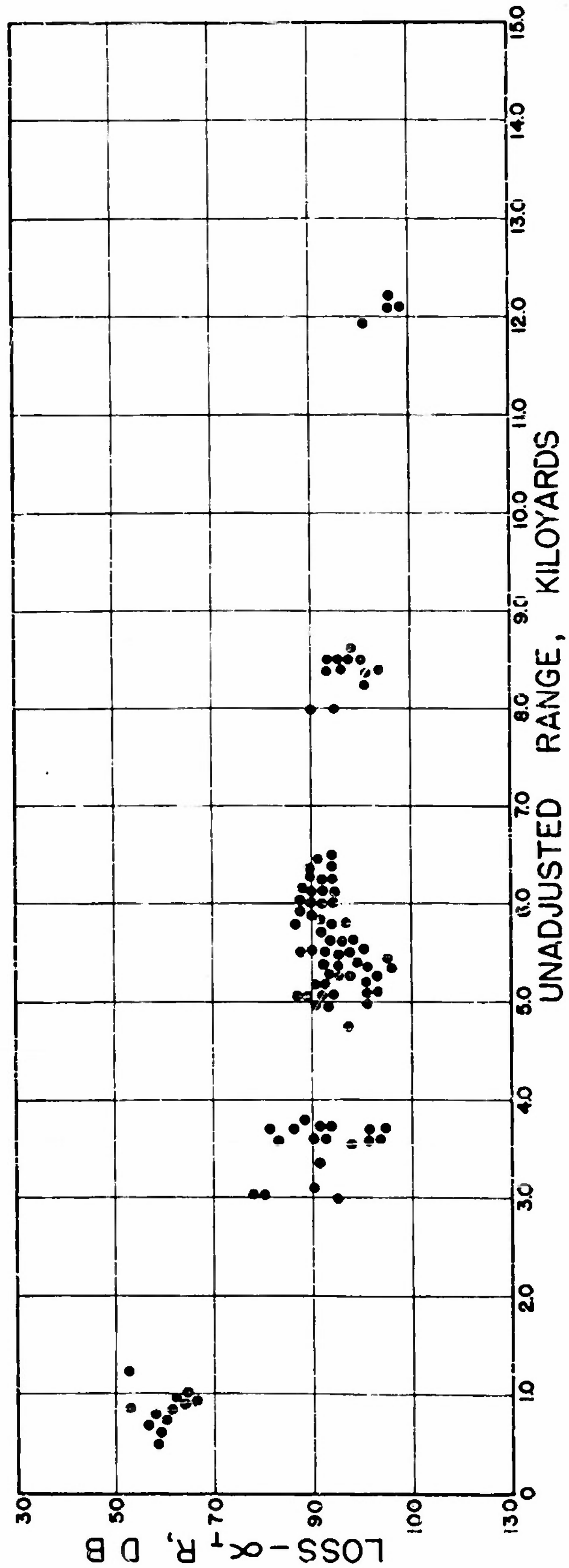

Fig. 9 Transmission Loss vs. Range for 8 kc and a Negative Gradient Extending Downward from the Surface

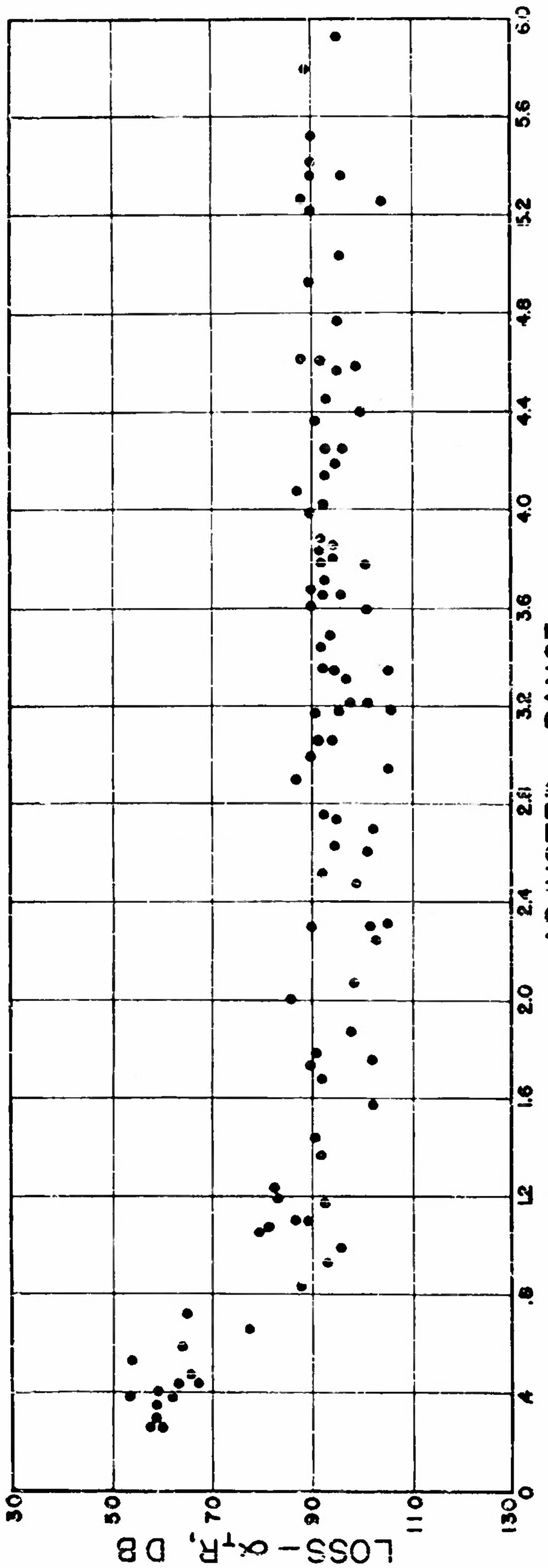

Fig. 10 Transmission Loss vs. Adjusted Range for 8 kc and a Negative Gradient Extending Downward from the Surface

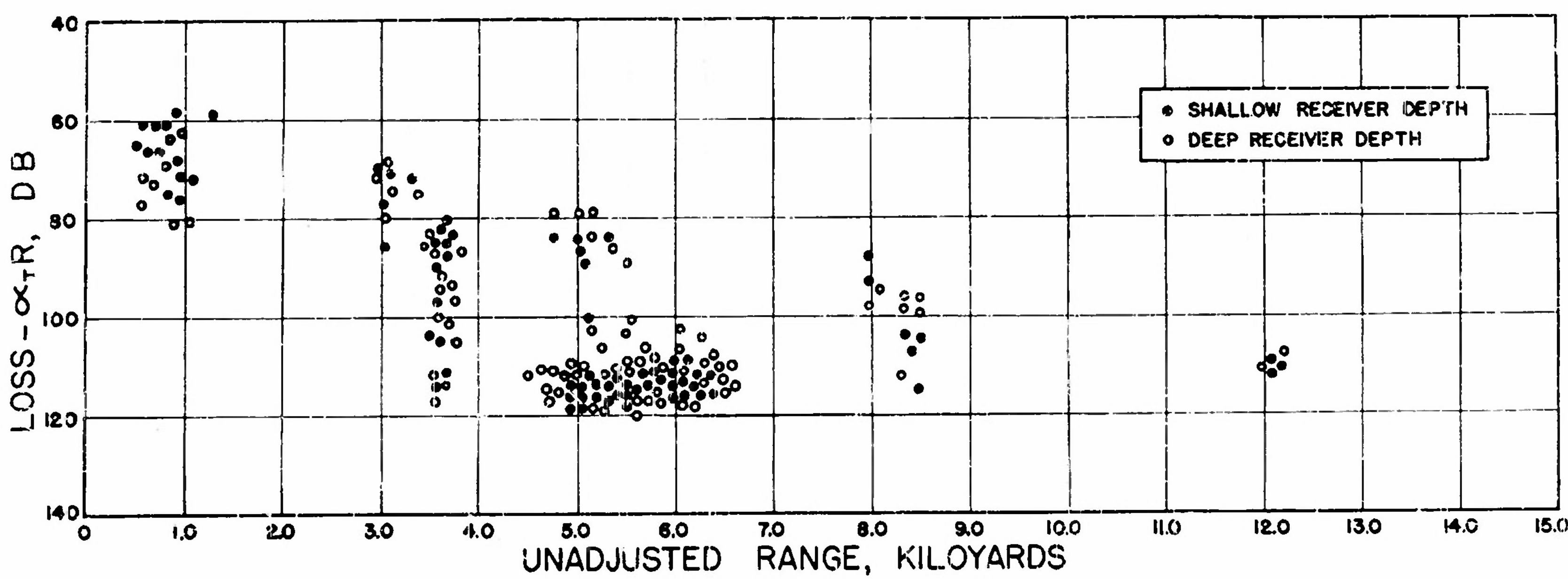

Fig. 11 Transmission Loss vs. Range for 25 kc and a Negative Gradient Extending Downward from the Surface

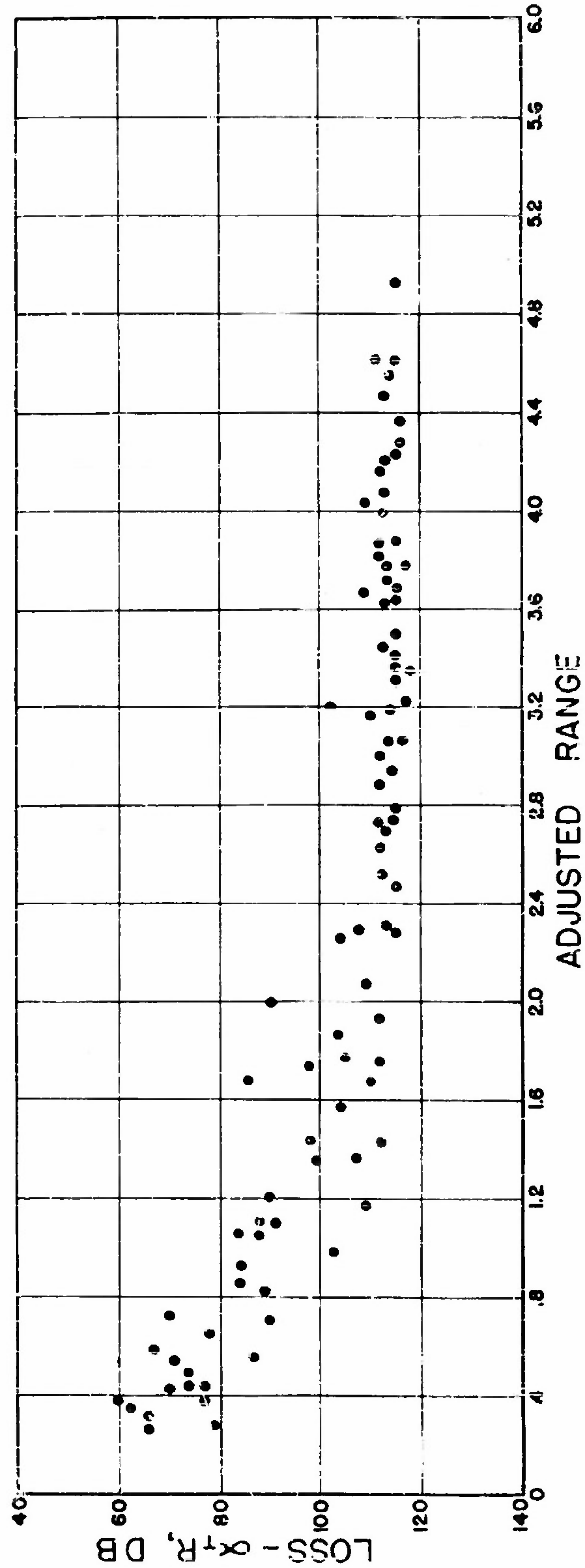

Fig. 12 Transmission Loss vs. Adjusted Range for 25 kc and a Negative Gradient Extending Downward from the Surface (Receiver Depths are 20 and 50 Feet)

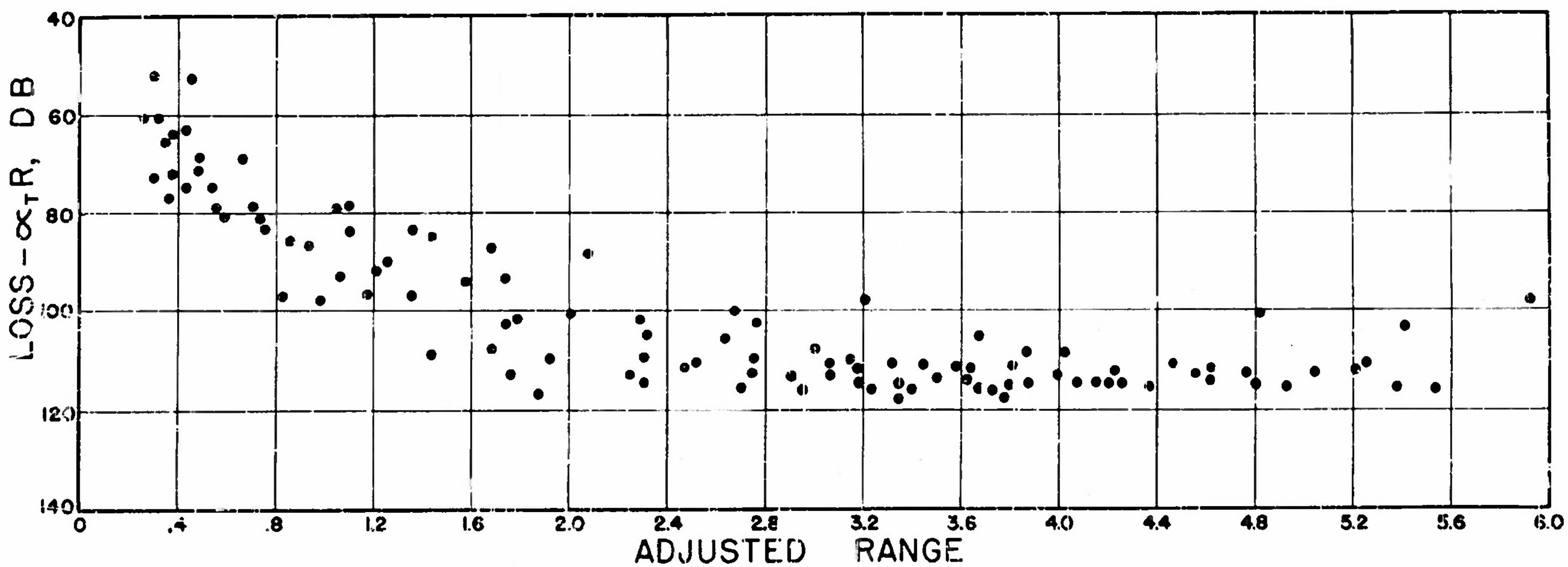

Fig. 13 Transmission Loss vs. Adjusted Range for 25 kc and a Negative Gradient Extending Downward from the Surface (Receiver Depths are 200 and 250 Feet)

In order to find out more about the mechanism by which sound is propagated into the shadow zone it would be of interest to (1) use pulse data, (2) study the effect of various parameters on the shape of the pulse received in the shadow zone, (3) study the rate of attenuation in the shadow zone for different conditions, and (4) determine the effect of frequency on the observed attentuation as a function of range.

VII. ANALYSIS OF SHALLOW WATER TRANSMISSION-LOSS DATA

In the period 1944 to 1945 the Woods Hole Oceanographic Institution made a number of shallow water sound transmission-loss measurements along the Atlantic coast and in the Gulf of Mexico with frequencies of 12 and 24 kc. The data were extensively analyzed and the results published in a WHOI memorandum.[10] A summary of part of the results appears in an NDRC Summary Technical Report.[11]

The most abundant data exist for propagation over sand bottoms with NAN and MIKE thermal conditions. Hence, to get results of statistical significance these were the categories on which most effort was spent. Table XIV shows the distribution of the transmission runs made by WHOI. Analyses of other types of bottoms are difficult because there is insufficient information as to the properties of various types with regard to reflection and absorption of sound.

In treating the data three adjustments were made to account for the following factors: (1) attenuation due to temperature-dependent relaxation effects, (2) bottom depth, and (3) the BT pattern.

The attenuation due to temperature-dependent relaxation effects was computed using the relationship

$$\alpha_{db/kyd} = A \frac{f^2 f_m}{f^2 + f_m^2} ,$$

where

f = frequency of sound wave,

[10] G. P. Woollard, "Sound Transmission Measurements at 12 kc and 24 kc in Shallow Water", WHOI, 1 May 1946 (Restricted).

[11] Summary Technical Report, Div. 6, vol. 8, 139-54, NDRC.

TABLE XIV

SUMMARY AND CLASSIFICATION OF WHOI OBSERVATIONS

	Sand	Sand Mud	Mud Sand	Mud	Stony	Deep 200 fms	Total
			24 kc				
NAN	47	20	11	25	16	-	119
CHARLIE	24	1	17	11	1	-	54
MIKE	33	4	6	28	18	-	89
PETER	7	13	2	44	-	6	72
			Steeply Sloping Bottoms				
UP SLOPE	-	6	-	-	-	-	6
DOWN SLOPE	4	-	-	12	-	-	16
	115	44	36	120	35	6	356
			12 kc				
NAN	36	12	7	16	15	1	87
CHARLIE	9	1	1	1	4	-	16
MIKE	32	2	-	19	2	-	55
PETER	9	12	5	45	-	7	78
			Steeply Sloping Bottoms				
UP SLOPE	-	6	-	6	-	-	12
DOWN SLOPE	1	-	-	12	-	-	13
	87	33	13	99	21	8	261
					GRAND TOTAL		617

$$f_m = 2.19 \times 10^7 \exp\left(\frac{-6300}{460 + t}\right),$$

$$t = \text{temperature, °F, and}$$

$$A = 0.61.$$

This is subtracted from the measured transmission loss at each range. The temperature used was an estimated average over the sound path.

For NAN patterns the adjustment for water depth was accomplished in two ways (1) by subtracting a term 10 log D from the measured transmission loss, and (2) by expressing the observed ranges in terms of the bottom skip distance. This is defined as the horizontal distance that a surface limited ray will travel between the point where it grazes the surface and the point that it strikes the bottom (Fig. 14).

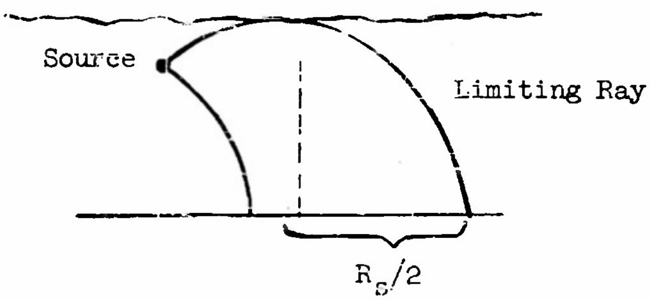

Fig. 14

Ray Diagram for Negative-Gradient Thermal Structure

The extent to which these adjustments have reduced the spread of the data may be seen from Figs. 15 and 16. These are plots of 24 kc transmission-loss data taken over sand bottoms under NAN-thermal conditions. Data are from 30 runs in 11 different areas. The average standard deviation has been reduced from 7 to 5 db. In selecting the 30 runs to be analyzed only those with no variations in the BT pattern with range were used.

Considerable effort was put into trying to find specific things that would account for the wide spread of the data that is found in transmission over the various types of bottoms, but with little success. More information is needed about such things as the reflective properties of the bottom, the horizontal thermal structure, thermal microstructure, and bottom contour. The amount of the Woollard data is inadequate to even arrive at any statistical conclusions.

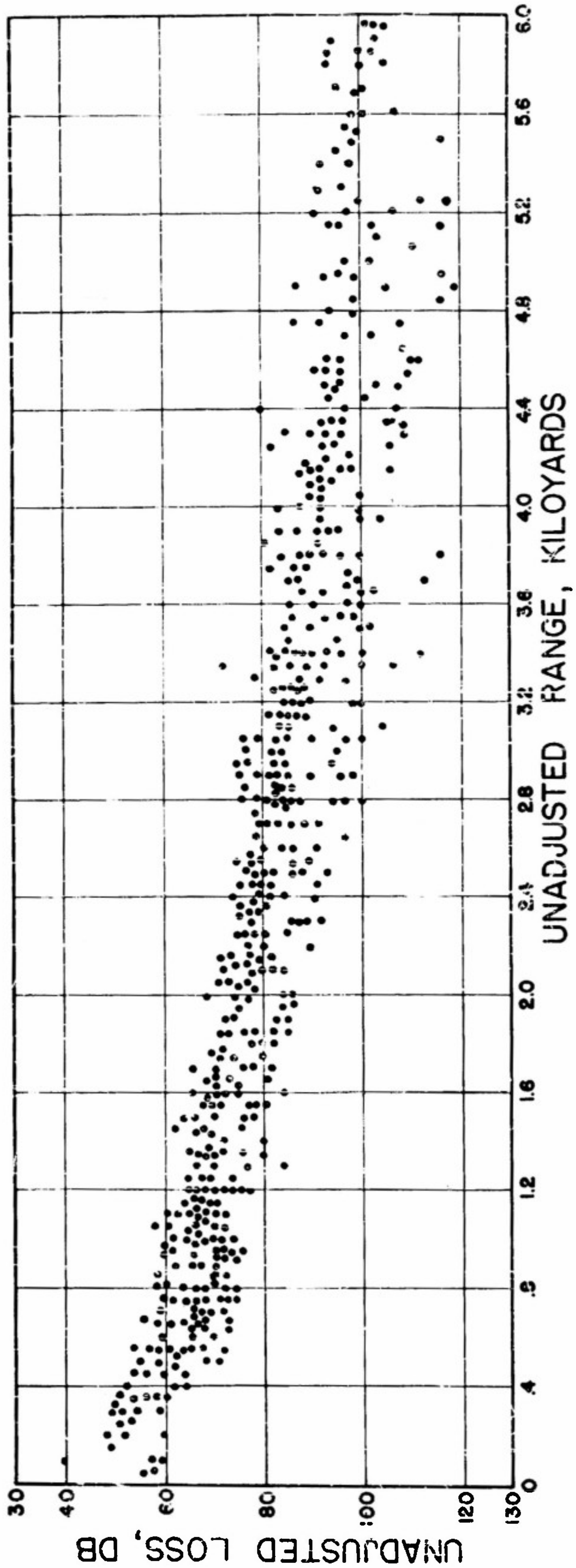

Fig. 15 Unadjusted Woollard Data for 24 kc, NAN Pattern, Sand Bottom, and Shallow Receiver

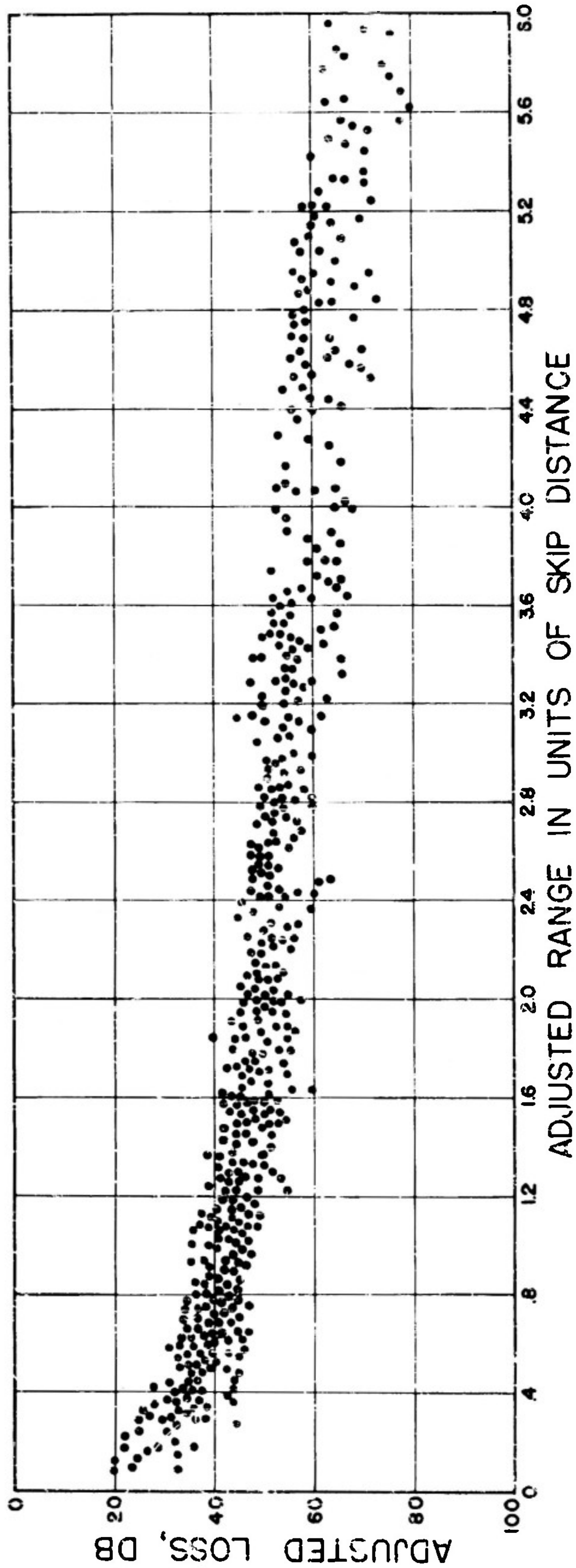

Fig. 16 Adjusted Woollard Data for 24 kc, NAN Pattern, Sand Bottom, and Shallow Receiver

VIII. A METHOD OF OBTAINING REFLECTION COEFFICIENTS OF THE SEA SURFACE FROM PULSE DATA

W. C. Meecham

The reflection coefficients of the surface can easily be determined from a study of pulse data, providing the transmitted pulse is short enough so that the direct and reflected components are separated and that only a small annular region of the surface is irradiated at any instant. These conditions will give a characteristic structure to the pulse which will enable the reflection coefficient of the surface to be calculated by the following method. Assume that:

(a) all contributions to the intensity measured have random phase,

(b) there is no volume scattering, and

(c) there is no true specular reflection.

For the purposes of simplicity only the cases where no refraction is present and the projector and the receiver are at the same depth will be considered. With a simple modification of the treatment it is possible to include these cases also.

If the sea surface is disregarded, then the contributions of the acoustic energy arriving at the receiver at any given instant after the direct pulse will be reflected from a surface of an ellipsoid of revolution with the projector and receiver at the two foci. If the sea surface is added, the points reflecting to the receiver form an ellipse on this surface, providing the projector and receiver are at the same depth z, as shown in Fig. 17. The energy arriving in the time interval, Δt, will be reflected from the zone between the ellipsoidal surfaces S_1 and S_2. This will begin to arrive at the receiver at a time t after the pulse was first transmitted,

$$t = \frac{r_o + r_1}{c} = \frac{\ell}{c} ,$$

r_o = range of scattering element from projector,

r_1 = range of scattering element from receiver,

c = velocity of sound propagation.

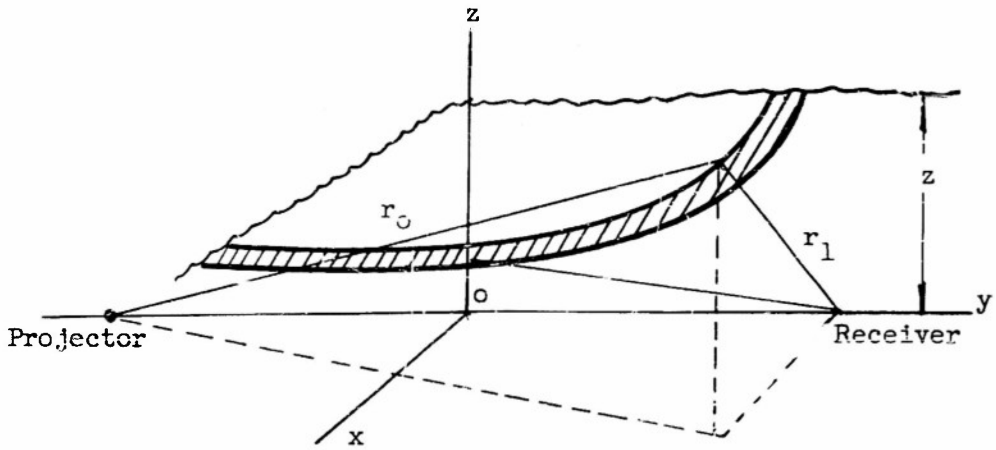

Fig. 17

Elliptical Zone on the Sea Surface Irradiated in a Time Δt

An instant later a new zone will be irradiated between S_2 and larger S_3 (not shown). Since random phasing between zones is assumed, each successive zone adds an increment ΔI to the average intensity. The increment in intensity can be expressed analytically as

$$\Delta I = \frac{1}{4\pi r_o^2} \frac{1}{4\pi r_1^2} \pi \frac{d}{d\ell} \left\{ \bar{a}(\ell)\, \bar{b}(\ell) \right\} c\, \Delta t\, \bar{A}\,(\theta,\phi;\theta',\phi') \quad ,$$

where

$\bar{A}(\theta,\phi;\theta',\phi')$ = reflection coefficient,

$\theta,\phi;\theta',\phi'$ = polar angles of the reflected and incident radiation, respectively, and

Δt = arbitrarily chosen increment of time.

The semimajor and semiminor axes, respectively, of the ellipsoid of revolution are $a(\ell)$ and $b(\ell)$. The coordinates of a point on the ellipse formed by the intersection of the sea surface and the ellipsoid of revolution are

$$\bar{a}(\ell) = a(\ell)\sqrt{1-\left(\frac{z}{b(\ell)}\right)^2}$$

and

$$\bar{b}(\ell) = b(\ell)\sqrt{1-\left(\frac{z}{b(\ell)}\right)^2}$$

where

$$a(\ell) = \frac{\ell}{2} ,$$

$$b(\ell) = 1/4 \sqrt{\ell^2 - r^2} ,$$

$$\ell = r_1 + r_o ,$$

r = range between the projector and the receiver.

Therefore, solving for the reflection coefficient and differentiating obtains

$$\bar{A}(\theta,\phi;\theta',\phi') = \frac{\Delta I}{c\Delta t} \frac{1}{F(\ell)} ,$$

where

$$F(\ell) = \frac{1}{16\pi r_o^2 r_1^2} \left[\sqrt{\ell^2 - r^2 - 4z^2} + \frac{\ell^2}{\sqrt{\ell^2 - r^2 - 4z^2}} \right] ,$$

and r = range between projector and receiver,

$$r^2 = 4(a^2 - b^2) .$$

An effort is being made to obtain suitable pulse data to test the method.

IX. VOLUME SCATTERING OF SOUND DUE TO SMALL RANDOM VARIATIONS IN THE INDEX OF REFRACTION

It is known that sound propagated in the sea undergoes volume scattering.[12] Liebermann has suggested that a possible source of the scattering is the small variations in the thermal structure of the sea.[13]

---

[12] "Physics of Sound in the Sea Part I Transmission", Div. 6, vol. 8, NDRC.

[13] Liebermann, L., J. of the Acous. Soc. of Amer. 23, 563 (1951).

Here the case of a plane wave passing through a medium containing random variations in the index of refraction is treated. It is assumed that the variations are caused by small inhomogeneities in the thermal structure.[13] Then an expression for the volume scattering coefficient m is obtained. By using certain experimentally measured quantities it is possible to calculate a value for m and compare it with the values reported in references 12 and 13.

First, consider a medium whose index of refraction is given by

$$\mu(\vec{r}) = 1 + \alpha n(\vec{r}) , \tag{1}$$

where

$$\alpha << 1,$$

and

$$\overline{n(\vec{r})} = 0 ,$$

$$\overline{n(\vec{r})\, n(\vec{r}\,')} = N(\vec{r} - \vec{r}\,') ,$$

$$N(0) = 0 .$$

α gives the rms variation of the refractive index, $N(\vec{r} - \vec{r}\,')$ is the auto-correlation function for variations in n, and $\overline{n(\vec{r})}$ indicates an average of $n(\vec{r})$ over the medium. In order to simplify the discussion, assume that $n(\vec{r}) = 0$ outside of a region of volume V.

The arguments and derivations are similar to those of Mintzer.[14] In the present work, plane instead of spherical waves are considered for simplicity and the scattering coefficient itself is derived.

Assuming an incident plane wave of unit intensity, the integral equation for the excess pressure is

$$p(\vec{r}) = e^{i\vec{k}_0\cdot\vec{r}} - \frac{2k_0^2\alpha}{4\pi} \int_V n(\vec{r}) \frac{e^{ik_0|\vec{r}-\vec{r}\,'|}}{|\vec{r}-\vec{r}\,'|} p(\vec{r}\,')\, d\vec{r}\,' . \tag{2}$$

[14] Mintzer, D., "Wave Propagation in a Randomly Inhomogeneous Medium I", Research Analysis Group, Brown University, 15 May 1953.

Since α is presumed small the Born approximation can be used and written for $p(\vec{r})$, the first term in the iteration expansion,

$$p(\vec{r}) = e^{i\vec{k}_o\cdot\vec{r}} - \frac{2k_o^2\alpha}{4\pi}\int_V n(\vec{r}\,')\,\frac{e^{ik_o|\vec{r}-\vec{r}\,'|}}{|\vec{r}-\vec{r}\,'|}\,e^{i\vec{k}_o\cdot\vec{r}\,'}\,d\vec{r}\,' . \tag{3}$$

If it is assumed that $n(\vec{r}) = 0$ for $|\vec{r}| > R$, then for $|\vec{r}| >> R$ it can be written

$$\frac{e^{ik_o|\vec{r}-\vec{r}\,'|}}{|\vec{r}-\vec{r}\,'|} \sim \frac{e^{ik_or}}{r}\,e^{-i\vec{k}\cdot\vec{r}\,'} ,$$

where $\vec{k} = k_o\frac{\vec{r}}{r}$. Therefore, for $|r| >> R$,

$$p(\vec{r}) = e^{ik_o\cdot\vec{r}} - \frac{2k_o^2\alpha}{4\pi}\int_V n(\vec{r}\,')\,e^{i(\vec{k}_o-\vec{k})\cdot\vec{r}\,'}\,dr'\,\frac{e^{ik_or}}{r} . \tag{4}$$

The scattering cross section is just the square of the absolute value of the coefficient of $\frac{e^{ik_or}}{r}$.

$$\sigma(\theta,\phi) = \left(\frac{k_o^2\alpha}{2\pi}\right)^2\left|\int_V n(\vec{r}\,')\,e^{i(\vec{k}_o-\vec{k})\cdot\vec{r}\,'}\,d\vec{r}\,'\right|^2$$
$$= \left(\frac{k_o^2\alpha}{2\pi}\right)^2\int_V\int_V d\vec{r}\,'\,d\vec{r}\,''\,n(\vec{r}\,')\,n(\vec{r}\,'')\,e^{i(\vec{k}_o-\vec{k})\cdot(\vec{r}\,'-\vec{r}\,'')} . \tag{5}$$

Here r" is the distance from the source to some other point in the scattering region. Now average over an ensemble of scatters to get the mean cross section and assume the ensemble average of $n(\vec{r}\,')\,n(\vec{r}\,'')$ is equal to the space average. The autocorrelation function is then

$$\langle n(\vec{r}\,')\,n(\vec{r}\,'')\rangle = \overline{n(\vec{r}\,')\,n(\vec{r}\,'')} = N(\vec{r}\,' - \vec{r}) .$$

Therefore,

$$\langle \sigma(\theta,\phi) \rangle = \left(\frac{k_0^2\alpha}{2\pi}\right)^2 \int_V d\vec{r}\,' \int_V d\vec{r}\,'' \, N(\vec{r}\,'-\vec{r}\,'') \, e^{i(\vec{k}_0-\vec{k}) \cdot (\vec{r}\,'-\vec{r}\,'')} \quad . \qquad (6)$$

Assume $N(\vec{r}\,'-\vec{r}\,'') \to 0$ for $|\vec{r}\,' - \vec{r}\,''| > \rho$, where ρ is small compared with the linear dimensions of the volume V and if variables are changed

$$\vec{r}\,' - \vec{r}\,'' = \vec{\xi} \ ,$$

$$\vec{r}\,' = \vec{r}\,' \ ,$$

then the $\vec{r}\,'$ integration will just introduce a factor of V and the $\vec{\xi}$ integration will be independent of the volume,

$$\langle \sigma(\theta,\phi) \rangle = V \left(\frac{k_0^2\alpha}{\alpha\pi}\right)^2 \int d\vec{\xi} \, e^{i(\vec{k}_0-\vec{k}) \cdot \vec{\xi}} \, N(\vec{\xi}) \ . \qquad (7)$$

Here the $\vec{\xi}$ integration may be taken over all space.

If written

$$N(\vec{q}) = \int d\vec{\xi} \, e^{i\vec{q}\cdot\vec{\xi}} \, N(\vec{\xi}) \ , \qquad (8)$$

where $q = |\vec{k}_0 - \vec{k}|$, the scattering coefficient $m(\theta,\phi)$, i.e., the fraction of the energy in a narrow beam which is scattered into the direction θ,ϕ per yard of travel, may be defined by

$$m(\theta,\phi) = \frac{1}{V} \langle \sigma(\theta,\phi) \rangle \ , \qquad (9)$$

then

$$m(\theta,\phi) = \left(\frac{k_0^2\alpha}{2\pi}\right)^2 N(\vec{k}_0 - \vec{k}) \ . \qquad (10)$$

Liebermann has measured the thermal microstructure in the ocean and states that the autocorrelation function for variations in the index of refraction due to these thermal fluctuations is approximated by the function

$$N(\vec{\xi}) = e^{-K\xi}, \qquad \xi = |\vec{\xi}| , \tag{11}$$

with $1/K \cong 60$ cm; he also quotes a value of $\alpha^2 = 5 \times 10^{-9}$.

Using Equation 11 it is found that

$$N(\vec{q}) = 8\pi \frac{K}{(K^2 + q^2)^2} , \tag{12}$$

and therefore,

$$m(\theta,\phi) = \frac{2}{\pi} \alpha^2 k_o^4 \frac{K}{(K^2 + |\vec{k}_o - \vec{k}|^2)^2} , \tag{13}$$

but $|\vec{k}_o - \vec{k}|^2 = 2k_o^2 (1 - \cos \theta)$ so

$$m(\theta,\phi) = \frac{2}{\pi} \alpha^2 \frac{k_o^4}{K^3} \left[1 + \frac{2k_o^2}{K^2} (1 - \cos \theta)\right]^{-2} , \tag{14a}$$

or

$$10 \log m(\theta,\phi) = 10 \log \frac{2}{\pi} \alpha^2 \frac{k_o^4}{K^3} - 20 \log \left[1 + \frac{2k_o^2}{K^2} (1-\cos \theta)\right] . \tag{14b}$$

For 24 kc sound $k_o = 90$ yd^{-1}. Using Liebermann's values of

$$K = 1.52 \text{ yd}^{-1}, \text{ and } \alpha^2 = 5 \times 10^{-9},$$

then

$$\frac{2}{\pi} \alpha^2 \frac{k_o^4}{K^3} \cong 6.2 \times 10^{-2} \text{ yd}^{-1},$$

and

$$10 \log \frac{2}{\pi} \alpha^2 \frac{k_o^4}{K^3} \cong -12. \text{ db} .$$

Therefore,

$$10 \log m(\theta,\phi) = -12 - 20 \log \left[1 + 7200 (1-\cos \theta)\right]$$

for $\theta = \pi$, i.e., back scattering and

$$10 \log m(\pi) \cong -95 \text{ db} .$$

From reverberation measurements as reported in reference 12

$$+ 10 \log m(\pi) = - 60 \pm 10 \text{ db}.$$

Clearly the observed thermal microstructure cannot account for the large reverberation in the ocean.

Mintzer's analysis puts definite limits on α^2/K, namely,

$$1.7 \times 10^{-9} \text{ yd} < \frac{\alpha^2}{K} < 1.7 \times 10^{-8} \text{ yd} .$$

Using $\alpha^2/K = 3 \times 10^{-9}$ yd it is found that if $10 \log m(\pi)$ is to be -60 db, then $k_o/K \cong 1$, and $1/K = 1$ cm. This is an order of magnitude smaller than Liebermann's value of K.

It is reported in reference 12 that the scattering coefficient for sound at angles between 10 and 120° is not more than about 10 db greater than back scattering. This is definitely not in agreement with the strong forward scattering that is predicted for thermal fluctuations. Hence, the actual scattering due to the thermal structure must be extremely small.

X. DERIVATION OF AN EQUATION FOR THE SCATTERING COEFFICIENT AND A CALCULATION OF IT FROM TRANSMISSION-LOSS DATA

When both a sound source and a receiver are omnidirectional in a horizontal plane in a sea which has a negative velocity gradient, it is possible to measure the volume scattering coefficient at a region of the ocean by placing the receiver in the shadow zone (see Fig. 16). In this paper a simple geometrical model is constructed and an expression for the scattering coefficient, m, is derived. Then suitable data are used to evaluate m.

A. Derivation of a Scattering Coefficient

First it is necessary to construct a simple geometric model for the ray patterns of the source and receiver. From Fig. 18 it is clear that only the sound scattered from the shaded region can reach the receiver. It is also evident that the maximum and minimum scattering angles for the sound reaching the receiver are those indicated.

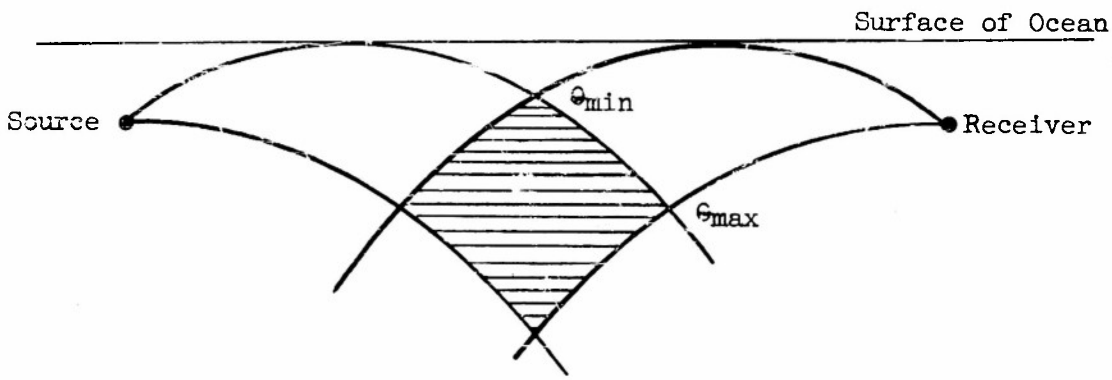

Fig. 18

Ray Diagram for Negative Thermal Gradients
(The shaded area is the region from which scattered energy will be picked up on the receiving hydrophone.)

It is possible to approximate the real situation by imagining the source and receiver to be in isovelocity water, but directed to make their rays meet at an angle θ_o, where θ_o is the "average" angle for the actual case (see Fig. 19).

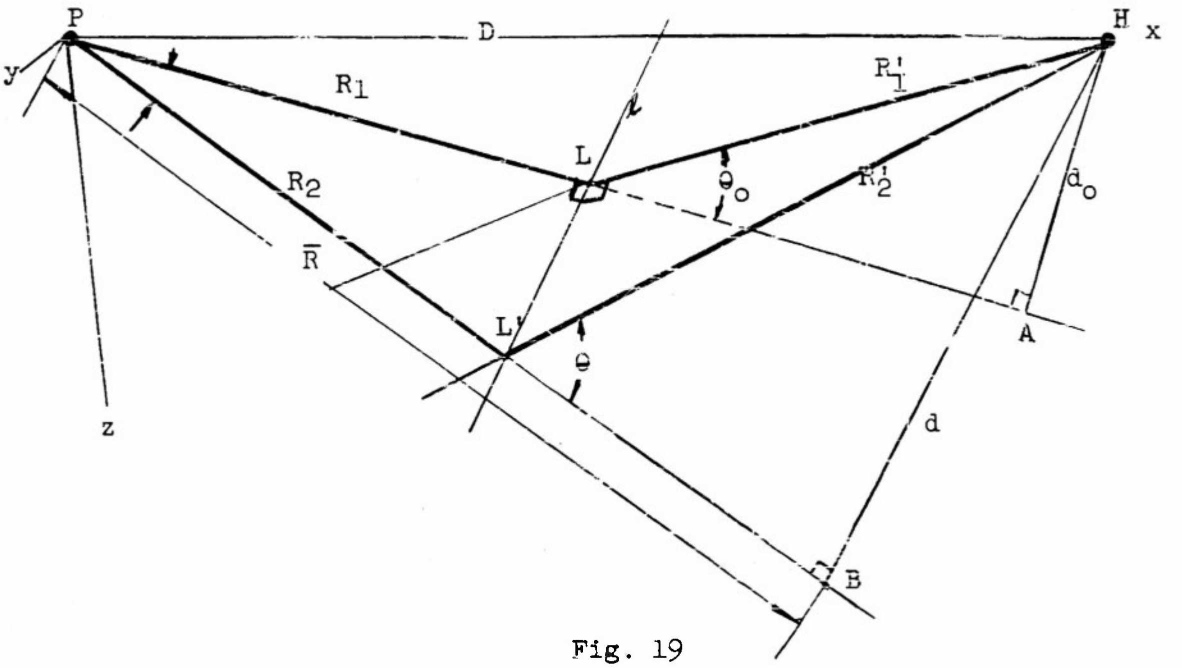

Fig. 19

Ray Diagram for Isovelocity Water

A sound beam from the source can be idealized lying between the two conical surfaces whose centers are at the source and which subtend an angle $\Delta\gamma_P$, determined by the vertical directivity of the transducer. The region from which the receiver can detect signals can similarly be considered as two intersecting planes making an angle $\Delta\gamma_H$ with respect to each other. The two sets of planes will intersect and enclose a common volume. The scattered energy reaching the receiver is assumed to come from this volume.

It is necessary at this point to introduce a list of definitions (see Fig. 12).

R = shortest distance between LL' and P,

R_1' = shortest distance between LL' and H,

d_o = shortest distance between ray PLH and H,

θ_o = angle between rays PLA and LH,

ϕ = angle between ray PLA and an arbitrary ray PB,

R_2 = distance from P to L' along ray PB,

R_2' = distance from L' to H,

θ = angle BL'H, and

d = shortest distance between ray PB and H.

If J is the energy flow per unit solid angle per second in the beam emitted by the source, then $J\Delta\gamma_p d\phi$ is the total energy in a narrow solid angle $\Delta\gamma_p d\phi$. The intensity of the sound scattered from the beam at an angle θ so it will reach the receiver while the sound traverses dR is

$$dI = \frac{J\Delta\gamma_p d\phi\; m(\theta)\; dR}{(R_2')^2}, \tag{15}$$

where $m(\theta)$ is the scattering coefficient for the angle θ.

It can be seen from Fig. 19 that

$$\bar{R} = R_2 + d \cot\theta,$$

differentiating

$$dR = d \csc^2\theta \, d\theta,$$

and since $R_2' = d \csc\theta$, Equation 15 can now be written in the form

$$\begin{aligned} dI &= \frac{J\Delta\gamma_p d\phi\; m(\theta)\; d\theta}{d} \\ &= \frac{J\Delta\gamma_p \Delta\gamma_H\; m(\theta)\; d\phi}{d}, \end{aligned} \tag{16}$$

since

$$d = d_o\sqrt{1 + \left(\frac{R_1 + R_1' \cos\theta_o}{d_o}\right)^2 \sin^2\phi}. \tag{17}$$

Equation 16 can be integrated and put in the form

$$I = \frac{J\Delta\gamma_p \, \Delta\gamma_H}{d_o} \int_{-\pi/2}^{+\pi/2} \frac{m(\theta)\, d\phi}{\sqrt{1 + \left(\frac{R_1 + R_1' \cos \theta_o}{d_o}\right)^2 \sin^2 \phi}} \,, \tag{18}$$

where I is the total intensity at the receiver.

Now if $m(\theta)$ is assumed independent of ϕ and Γ is defined as

$$\Gamma = \frac{1}{\pi} \int_{-\pi/2}^{+\pi/2} \frac{d\phi}{\sqrt{1 + \left(\frac{R_1 + R_1' \cos \theta_o}{d_o}\right) \sin^2 \phi}} \,, \quad \Gamma \leqq 1 \,, \tag{19}$$

then

$$I = \frac{\pi J \, \Delta\gamma_p \, \Delta\gamma_H \, \overline{m(\theta)}}{d_o} \, \Gamma \,. \tag{20}$$

Γ is a geometrical factor which depends on the spreading of the beam. $\Gamma = 1$ corresponds to the "narrow" beam which moves along ray PLA in Fig. 12.*

B. Determination of the Value of m from Deep Water Negative-Gradient Transmission Data

It is now possible to write Equation 20 in the form

$$-10 \log m = \text{measured loss} + 10 \log \frac{\Delta\gamma_p}{\pi} + 10 \log \frac{\Delta\gamma_H}{\pi} + 10 \log \Gamma + 30 \log \pi - 10 \log d_o - \alpha_I R \,, \tag{21}$$

*For $\Gamma = 1$, Equation 20 corresponds to Equation 18 on page 127 of "Physics of Sound in the Sea", Part 1 NDRC-STR, Div. 6, vol. 8.

where "measured loss" is $-10 \log I/J$. α_T is the temperature-dependant attenuation coefficient.

Using Equation 21 and data with definite negative-velocity gradients from six stations of AMOS Cruises 5,8,9, and 11, values of $-10 \log m$ were found. The results varied from 35 to 75 db. The geometric values R_1, d_o, θ_o, and R_1' were obtained from the actual ray diagrams. These values are a fair approximation of the values in the geometric model, since $\log \Gamma$ is insensitive to changes in R_1, d_o, θ_o, and R_1'. The Γ's were evaluated graphically.

C. Discussion

The large variation found in the scattering coefficient could be due to one or more of several things (1) the model, (2) unknown causes of scattering (i.e., organic material), or (3) temperature variations in the sea.

From the model used m might be expected to be too large, but it is not obvious that it would cause such drastic variations. The tendency, therefore, would be to conclude that the model is satisfactory. A better model, however, was attempted using two sets of intersecting cones instead of disks. The integral over the volume included in the region of intersection of the cones is very difficult and was not solved.

It is known that biological layers exist in the oceans and can cause appreciable scattering.[15] This was considered as a possible source of the variation in m. If a scattering layer is present in the allowed zone for the receiver (see Fig. 11), then a large value of m might be found. The scattering layers are known to migrate diurnally,[16] which would give rise to variations in m. For this reason an attempt was made to find a day-night variation in the data. It appeared that this variation was present, although the amount of data was not large enough to be definite. More investigation of this explanation is intended. A definite correlation could be attempted on the variation of m with the presence of a scattering layer if loss measurements were taken simultaneously with direct reverberation measurements. In this way the presence and depth of the scattering layer would be known for all loss measurements.

Temperature variations were studied in section IX of this report and it was seen that small local variations could not account for a value of $m > 10^{-8}$.

---

[15] NEL Report 334, 8 January 1953 (Unclassified).

[16] "Principles of Underwater Sound", Div. 6, vol. 7, Ch. 5, NDRC.